EC Principles: Physics Overview

NAGASAKI Kazunobu (長崎 百伸)

Institute of Advanced Energy, Kyoto University, Japan

What Are ECH and ECCD?

- Electron cyclotron heating (ECH) and current drive (ECCD) are one of the most powerful and highly controllable methods for plasma heating and current drive in magnetic confinement devices
- ECH/ECCD operates on the principle of resonance between an injected EM wave and the gyration of electrons around the magnetic field
- The wave frequency: **10-300 GHz (30mm - 1mm)**
- The injected power: **0.1 - 10 MW** at existing devices

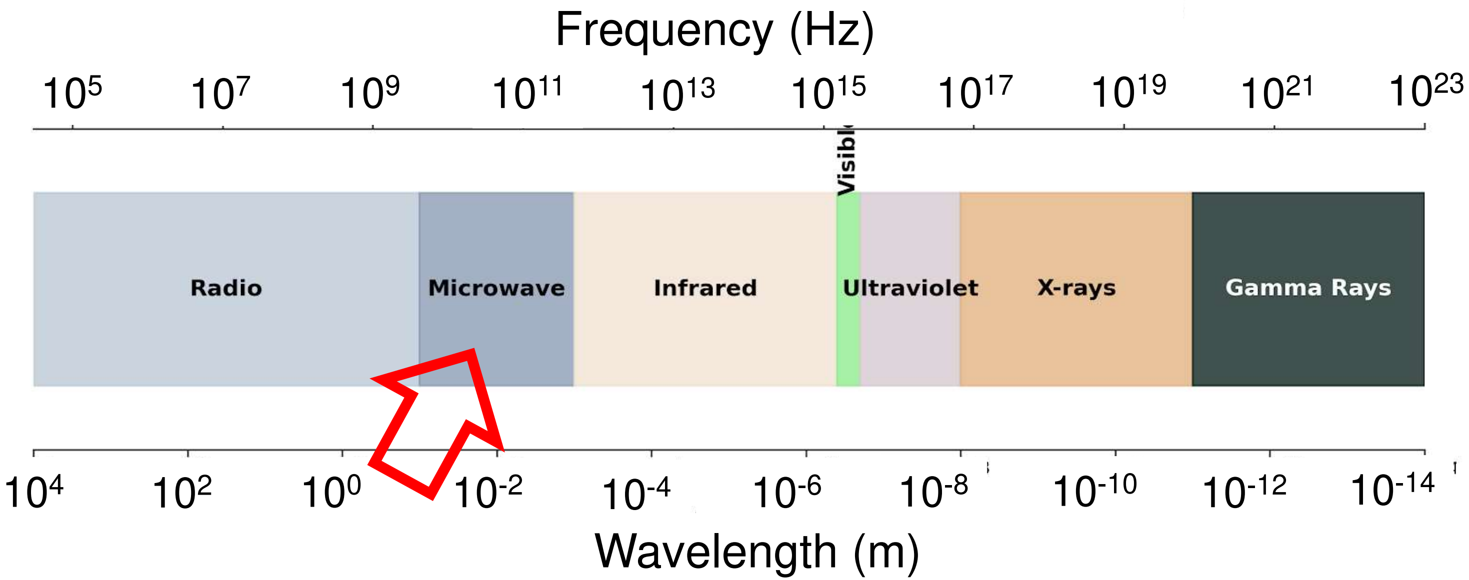

Heating/Current Drive (H/CD) system is mandatory for ITER and DEMO reactor

- Accessing the steady-state regime
  - Plasma startup
  - Heating for D-T burn
  - H-mode access
  - Control of current profile for high performance operation
- Steady-state sustainment
  - Full non-inductive operation
  - Stable operation
- Plasma control
  - Impurity
  - MHD instabilities (sawtooth, NTM, RWM, AE)

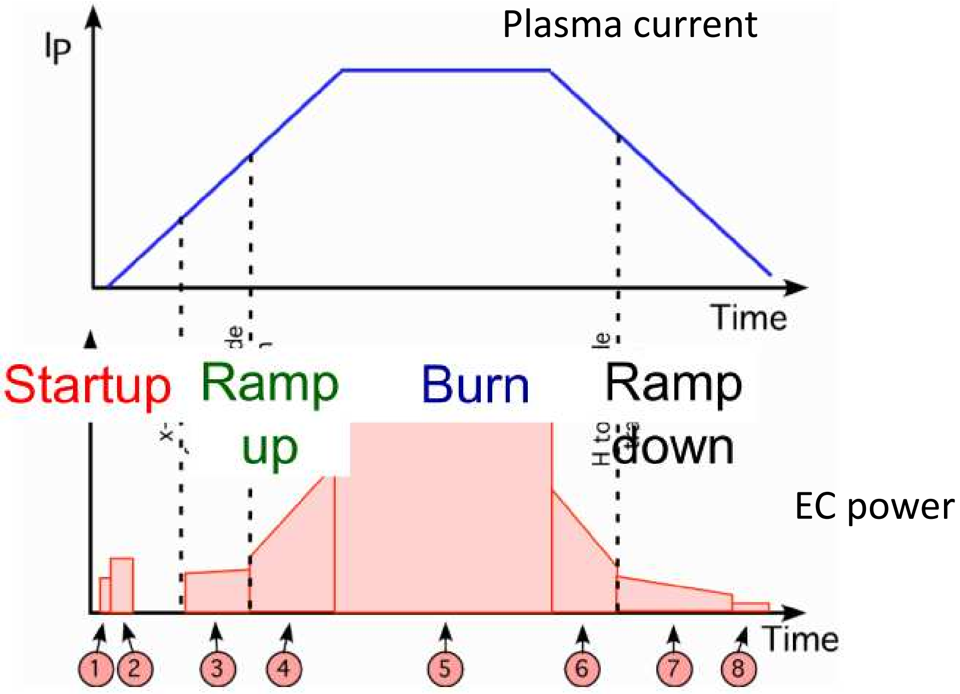

Franke, Fus. Eng. Design (2017)

Pros and Cons of ECH/ECCD

Pros

- Effective source of highly localized and controlled heating and current drive
- Easy coupling to plasma because of wave propagation in vacuum
- Small antennas (high power density 100 MW/m^2)
- Well-developed EC technology (gyrotron, transmission and launcher)
- Theory validated by experiment

Cons

- No direct ion heating
- Accessible density limit
- Low current drive efficiency compared to other methods like LHCD and NBCD
- More technology reliability for high power (~100 MW) steady-state (> 1000 sec) operation

Outline

1. Fundamentals of Electron Cyclotron Waves
2. Wave Propagation & Accessibility
3. Wave absorption
4. Ray tracing simulation
5. Electron cyclotron current drive (ECCD)
6. Applications

Fundamentals of Electron Cyclotron (EC) Waves

Electron Cyclotron Frequency

The Lorentz force governs electron motion in a static magnetic field:

$$\boldsymbol{F} = -e\left(\boldsymbol{E} + \boldsymbol{v} \times \boldsymbol{B}_0\right)$$

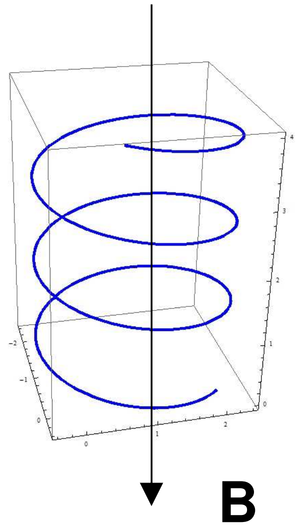

Electrons gyrate around the magnetic field.

The electron cyclotron frequency is given by

$$\boxed{\omega_{ce} = \frac{eB_0}{m_{e0}\gamma}} \qquad \gamma = \left(1 - \frac{v^2}{c^2}\right)^{-\frac{1}{2}}$$

Lorentz factor

$$f_{ce} = 28 B_0 \ [\mathrm{GHz}]$$

f_{ce} = 28 GHz for 1T

f_{ce} = 148 GHz for 5.3T

Millimeter wave range, λ = 1-30 mm

Plasma Frequency

Plasma oscillation (often called a Langmuir wave) is the fundamental, rapid oscillation of electron density in a plasma. It is one of the most basic and vital collective behaviors that defines the plasma state.

$$\boxed{\omega_{pe} = \sqrt{\frac{n_e e^2}{m_e \varepsilon_0}}}$$

$$f_{pe} = 28\sqrt{\frac{n_e}{10^{19}}} \ \text{[GHz]}$$

f_{pe} = 28 GHz at $n_e = 10^{19}$ m^{-3}

f_{pe} = 89 GHz at $n_e = 10^{20}$ m^{-3}

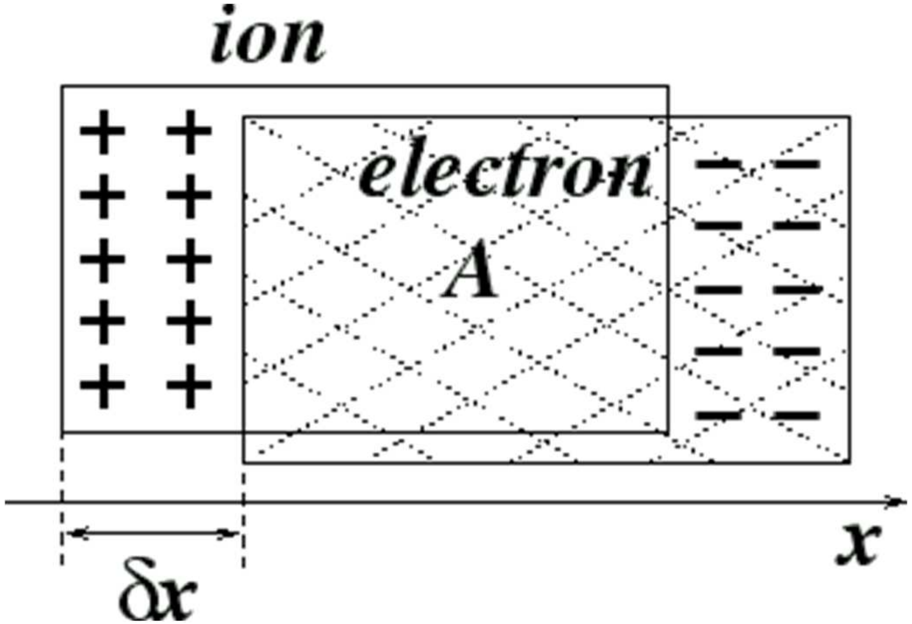

Electrons displaced from ions oscillate at ω_{pe} due to the electrostatic restoring force.

Electron Cyclotron Resonance

The spiral motion of electrons interacts with electromagnetic waves, resulting in the conversion of wave energy into the kinetic energy of the electrons.

$$\boxed{\omega - k_{\parallel} v_{\parallel} = n\omega_{ce}}$$

ω: Wave angular frequency

$k_{\parallel}$: Wave vector parallel to B

$v_{\parallel}$: Electron velocity parallel to B

n: Harmonic number ($n = 1,2,3, \ldots$)

- k∥ v∥: Doppler shift — extends resonance to a layer, not a surface
- 1/γ: relativistic mass increase shifts resonance inward

Both the **Doppler shift** and **relativistic effect** (γ) modify where resonance occurs.

Electron Cyclotron Resonance Condition

Resonance condition

$$\omega - k_{\parallel} v_{\parallel} = n\omega_{ce}$$

Normalized resonance condition
in velocity space

$$\boxed{\frac{\left(u_{\parallel} - u_{\parallel 0}\right)^2}{\alpha_{\parallel}^2} + \frac{{u_{\perp}}^2}{\alpha_{\perp}^2} = 1}$$

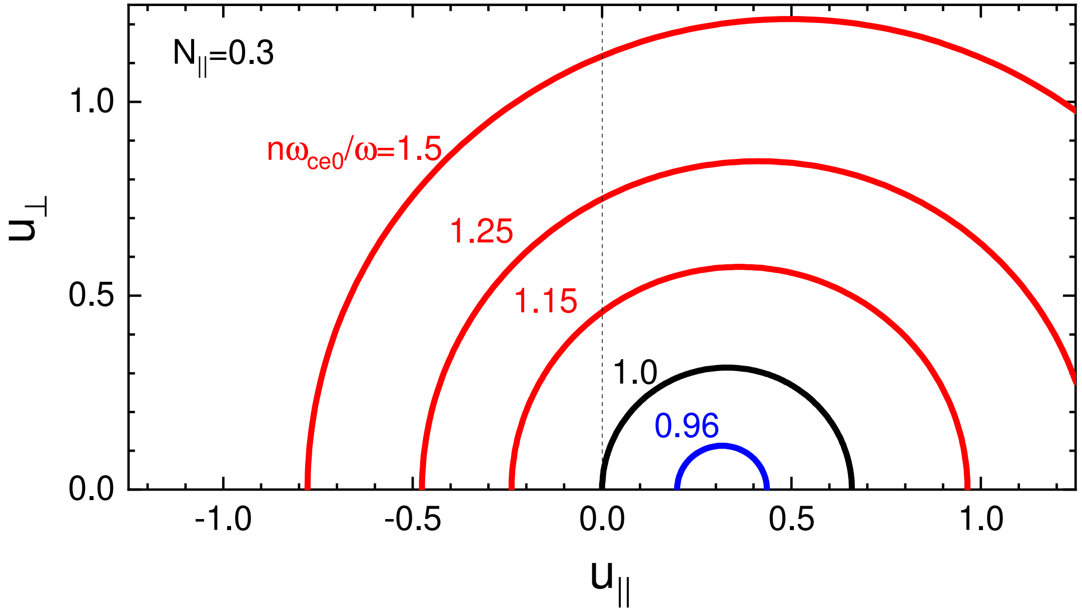

$$u_{\parallel 0} = \frac{N_{\parallel}}{1 - {N_{\parallel}}^2} \frac{n\omega_{ce}}{\omega},$$

$$\alpha_{\parallel} = \frac{\sqrt{{N_{\parallel}}^2 + (n\omega_{ce}/\omega)^2 - 1}}{1 - {N_{\parallel}}^2}, \quad \alpha_{\perp} = \frac{\sqrt{{N_{\parallel}}^2 + (n\omega_{ce}/\omega)^2 - 1}}{\sqrt{1 - {N_{\parallel}}^2}}$$

Doppler Shift and Relativistic Effect

- The radial position and width of power absorption profile depend on the Doppler shift and relativistic effect in the resonance condition, $\omega - k_{\parallel} v_{\parallel} = n\omega_{ce}$
- The profile width is wider with an increase in $N_{||}$ and T_e

Doppler shift

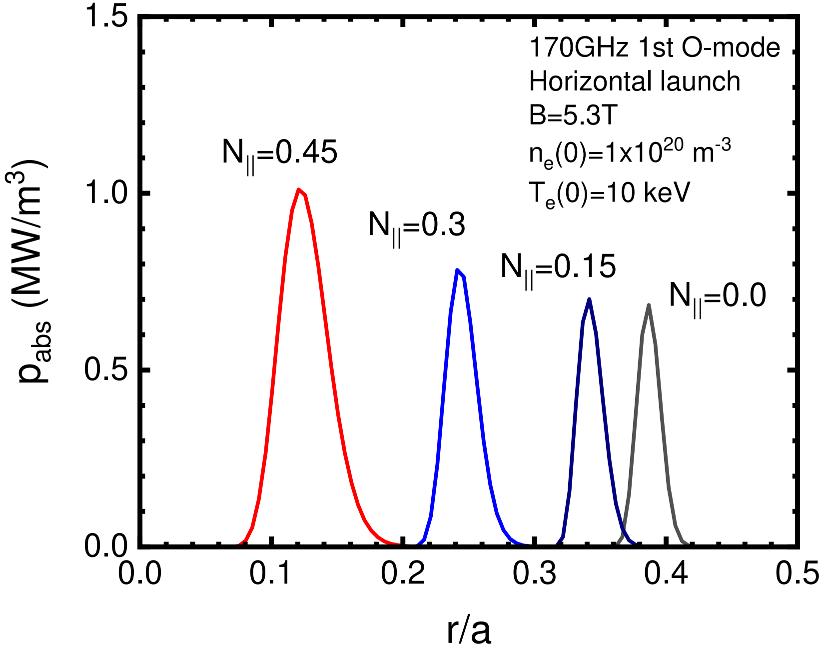

Relativistic effect

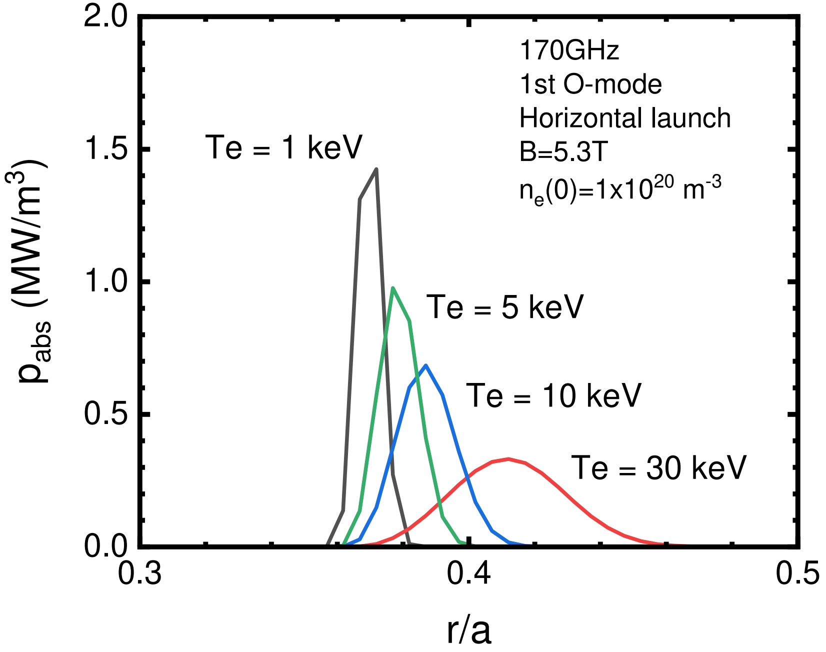

Wave Propagation & Accessibility

Wave Equation for EC Waves

Maxwell's equations

$$\nabla\times\mathbf{E}_1=-\frac{\partial\mathbf{B}_1}{\partial t}$$

$$\nabla\times\mathbf{B}_1=\frac{1}{c^2}\frac{\partial\mathbf{E}_1}{\partial t}+\mu_0\mathbf{J}_1$$

From above equations,

$$\nabla\times\nabla\times\mathbf{E}_1=-\left(\frac{1}{c^2}\frac{\partial\mathbf{E}_1}{\partial t}+\mu_0\frac{\partial\mathbf{J}_1}{\partial t}\right)$$

Fourier decomposing and assuming field perturbation $\exp[i(\mathbf{k}\cdot\mathbf{x}-\omega t)]$, and $\mathbf{N}=c\mathbf{k}/\omega$,

$$\boxed{\mathbf{N}\times\mathbf{N}\times\mathbf{E}_1+\mathbf{K}\cdot\mathbf{E}=0}$$

Dielectric tensor

$$\mathbf{E}_1+\frac{i\mathbf{J}_1}{\varepsilon_0\omega}=\mathbf{K}\cdot\mathbf{E}_1$$

Current that flows in the plasma

$$\mathbf{J}_1=-en_0v_{1e}$$

Momentum equation

$$en_0m_e\frac{\partial\mathbf{v}_{1e}}{\partial t}=-en_0\left(\mathbf{E}_1+\mathbf{v}_{1e}\times\mathbf{B}_0\right)$$

Dispersion Relation of EC Waves in "Cold" Plasma

Equations for waves

$$\begin{bmatrix} S-N^2\cos^2\theta & -iD & N^2\cos\theta\sin\theta \\ iD & S-N^2 & 0 \\ N^2\cos\theta\sin\theta & 0 & P-N^2\sin^2\theta \end{bmatrix}\begin{bmatrix} E_x \\ E_y \\ E_z \end{bmatrix}=0$$

$$P=1-\frac{\omega_{pe}{}^2}{\omega^2}$$

$$R=1-\frac{\omega_{pe}{}^2}{\omega^2}\frac{\omega}{\omega-\Omega_e}$$

$$L=1-\frac{\omega_{pe}{}^2}{\omega^2}\frac{\omega}{\omega+\Omega_e}$$

$$S=\frac{R+L}{2}$$

$$D=\frac{R-L}{2}$$

Appleton-Hartree equation

$$\boxed{AN^4-BN^2+C=0}$$

$$A=S\sin^2\theta+P\cos^2\theta$$

$$B=RL\sin^2\theta+PS(1+P\cos^2\theta)$$

$$C=PRL$$

$$\tan^2\theta+\frac{P\left(N^2-R\right)\left(N^2-L\right)}{\left(SN^2-RL\right)\left(N^2-P\right)}=0$$

Two electromagnetic modes

- Ordinary (O) mode
- Extraordinary (X) mode

Ordinary (O) Mode at θ=π/2

Dispersion Relation

$$\boxed{N_\perp{}^2 = 1 - \frac{\omega^2}{\omega_{pe}^2}}$$

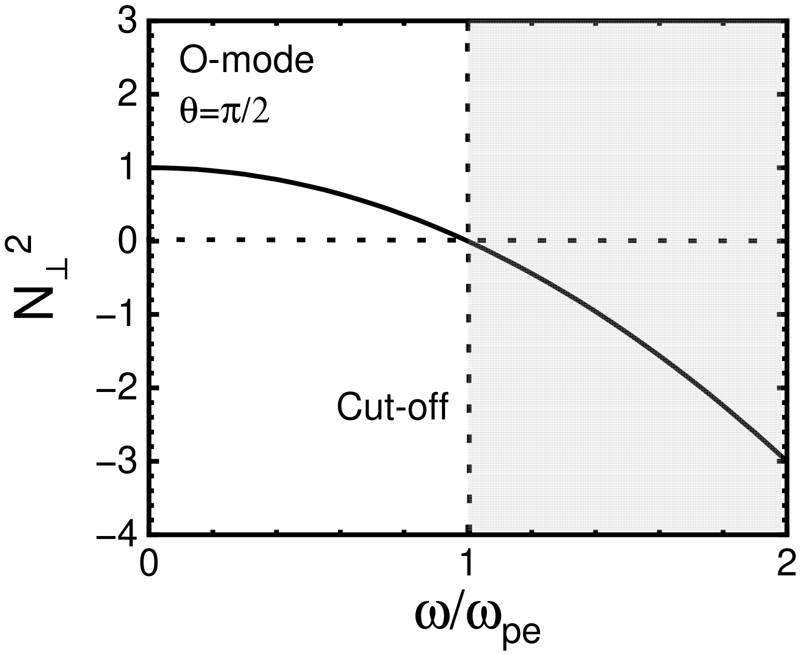

Polarization:

Linear with $E_1 \| B_0$

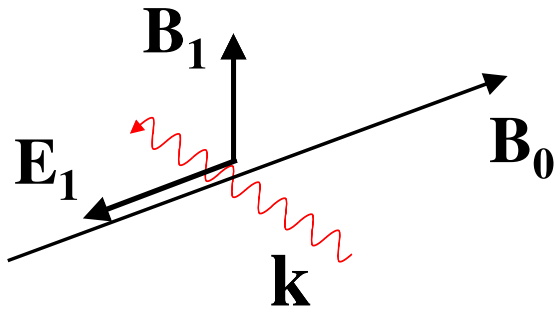

Wave Cutoff: $N_\perp{}^2 = 0$

Critical density limit

$$n_e^{crit} = \left(\frac{f}{28\times10^9}\right)^2 \ [m^{-3}]$$

If ne exceeds this threshold,
the wave cannot penetrate and reflects.

Extraordinary (X) Mode at θ=π/2

Dispersion Relation

$$\boxed{N_\perp{}^2 = 1 - \frac{\omega_{pe}^2\left(\omega^2 - \omega_{pe}^2\right)}{\omega^2\left(\omega^2 - \omega_{UH}^2\right)}}$$

$$\omega_{UH}^2 = \omega_{pe}^2 + \omega_{ce}^2$$

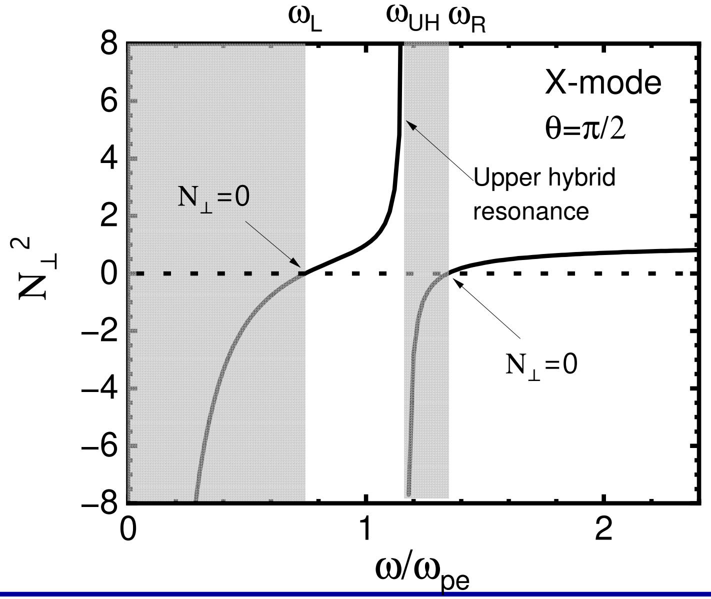

Polarization:

Elliptical

in the plane perpendicular to B_0

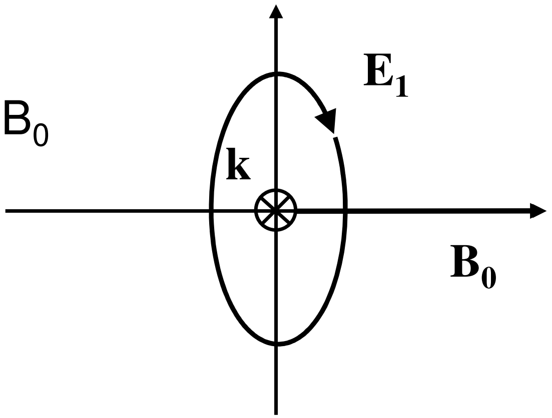

Wave Cutoff: $N_\perp{}^2 = 0$

$$\omega_L = \frac{-\omega_{ce} + \sqrt{\omega_{ce}{}^2 + 4\omega_{pe}{}^2}}{2}$$

$$\omega_R = \frac{\omega_{ce} + \sqrt{\omega_{ce}{}^2 + 4\omega_{pe}{}^2}}{2}$$

If ne exceeds this threshold,
the wave cannot penetrate and reflects .

Radial Profiles of EC-Related Frequencies

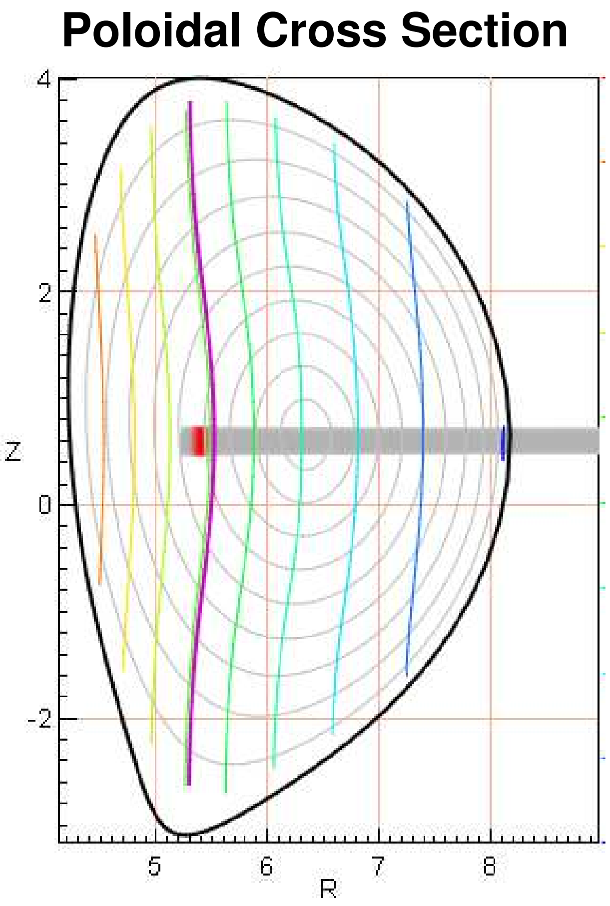

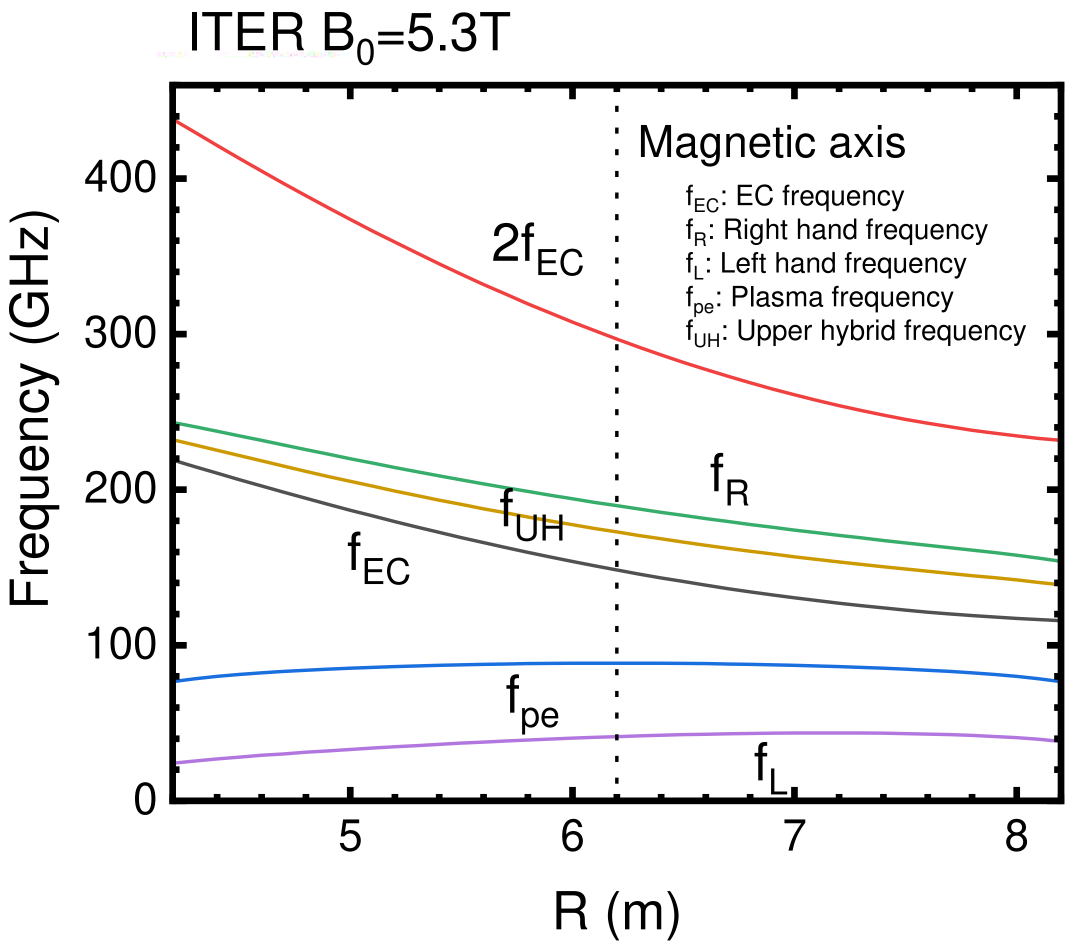

O-mode Propagation

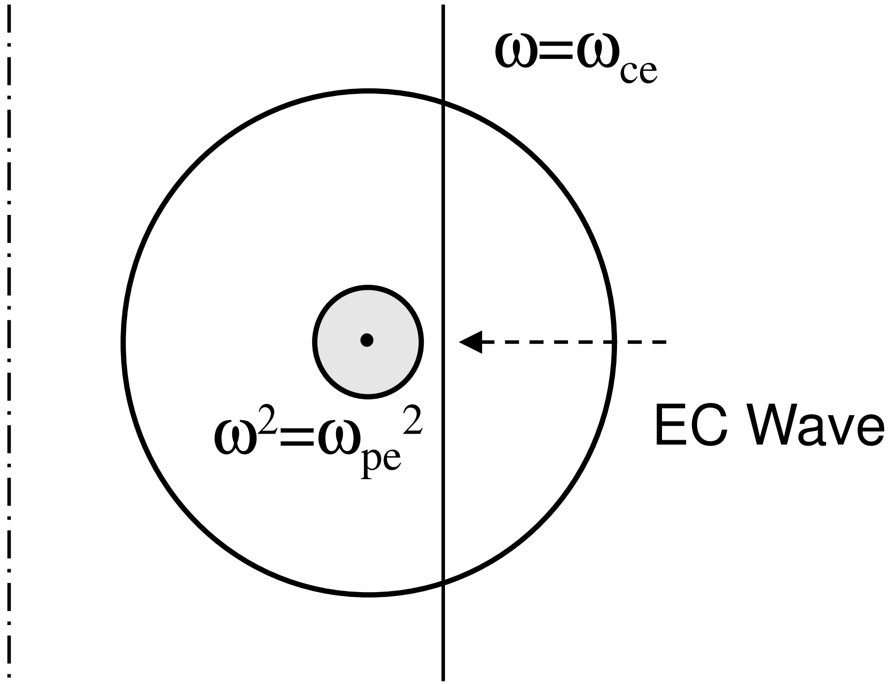

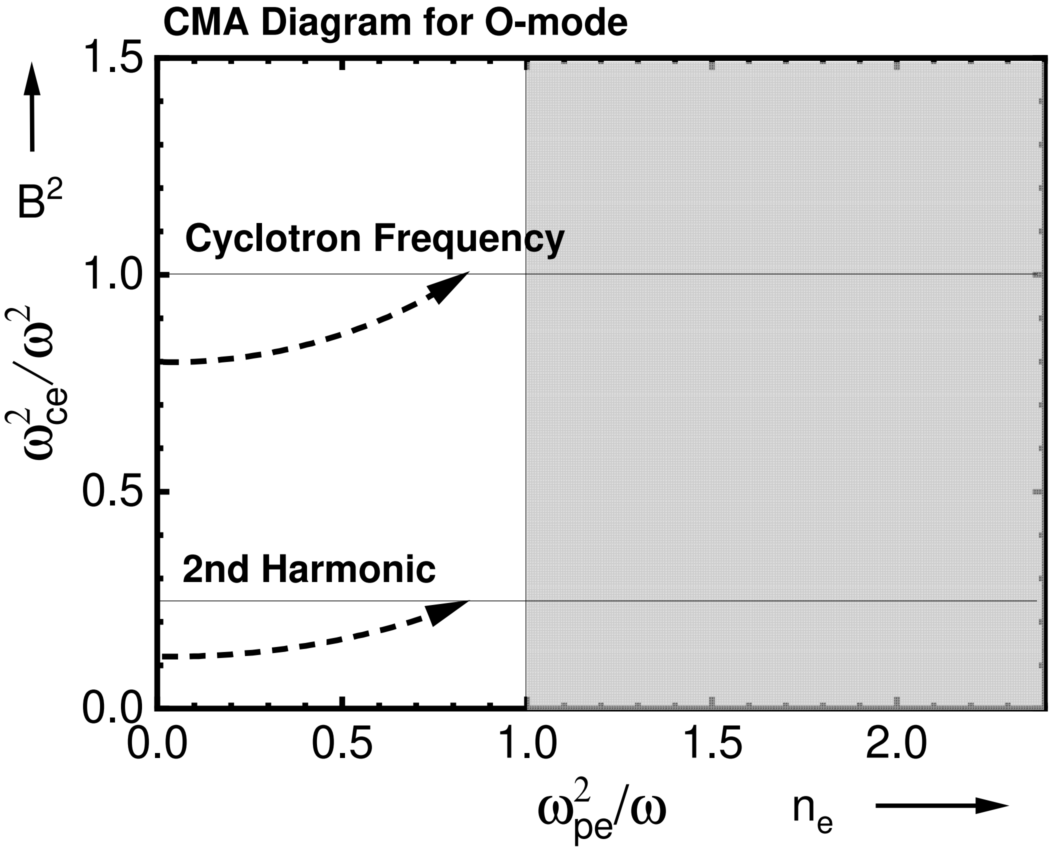

X-mode Propagation

Fundamental

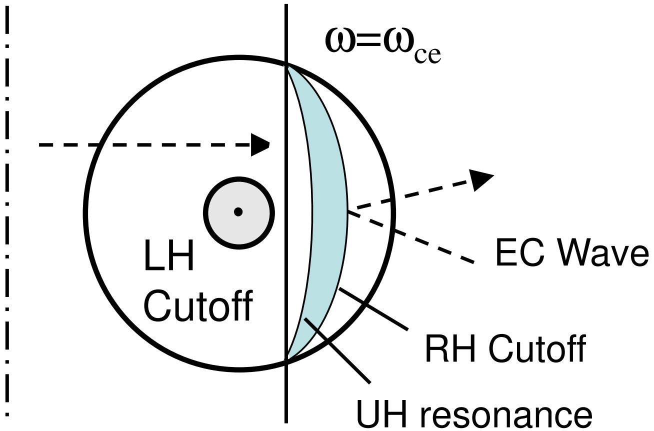

2nd Harmonic

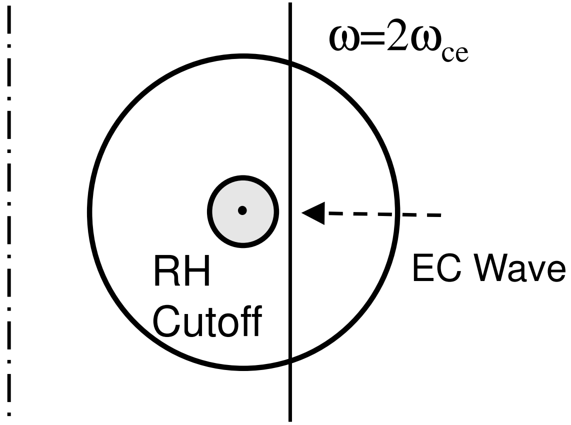

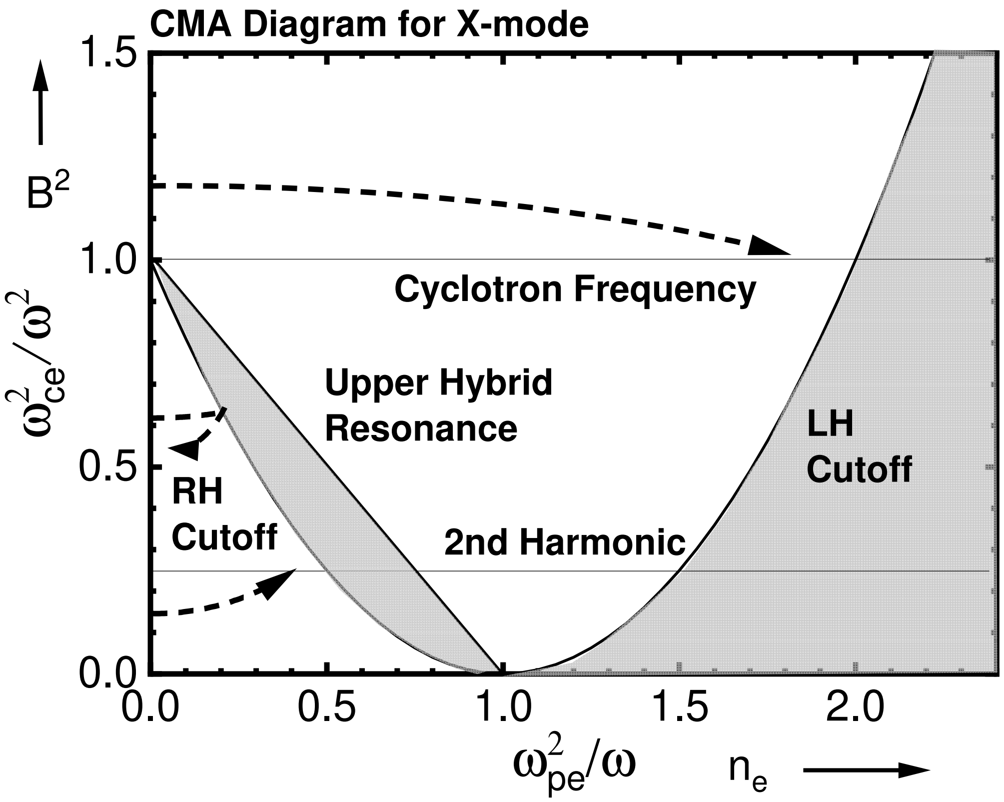

Wave Absorption

Governing Equations for Absorption

Radiation transfer equation

$$N^2 \frac{d}{ds}\left(\frac{I_\omega}{N^2}\right) = j_\omega - \alpha_\omega I_\omega$$

I_ω: Radiation intensity
j_ω: Emission coefficient

$$E = E_0 \exp i\left(\mathbf{k}\cdot\mathbf{r} - \omega t\right)$$
$$= E_0 \exp\left(-k_i x\right) \exp i\left(k_r x - \omega t\right)$$

Absorption coefficient

$$\boxed{\alpha_\omega = 2\,\mathrm{Im}\left(k\right) = 2k_i}$$

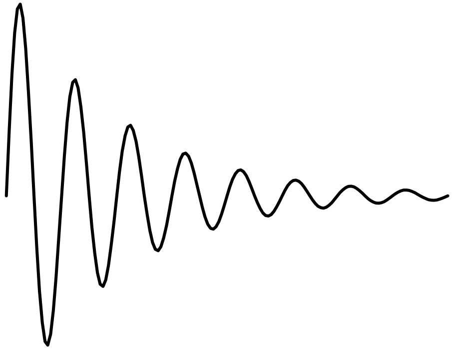

$$k = k_r + ik_i$$

- Formulate the wave equation from Maxwell's equations.
- Calculate $\mathbf{J}$ using the linearized Vlasov equation to obtain the hot plasma dielectric tensor $\boldsymbol{\varepsilon}$.
- Solve the dispersion relation for k.

Physical Mechanism of X2-Mode Heating

Electron position: $\mathbf{r} = \left(\rho\cos 2\omega_{ce}t,\ \rho\sin 2\omega_{ce}t\right)$

Wave electric field: $E_x = E_{x1}e^{i(\mathbf{k}\cdot\mathbf{r}-\omega t)}$

$$E_{x1}e^{i(\mathbf{k}\cdot\mathbf{r}-\omega t)} = E_{x1}e^{i(k_\perp\rho_e\cos 2\omega_{ce}t-\omega t)} = E_{x1}\sum_{n=-\infty}^{\infty} i^n J_n\left(k_\perp\rho_e\right)e^{i(2n\omega_{ce}-\omega)t}$$

If $\omega=2\,\omega_{ce}$,

$$\left\langle E_x\right\rangle = -E_{x1}J_2\left(k_\perp\rho_e\right)$$

Averaged electric field is finite!

Since $k_\perp\rho_e \ll 1$,

$$\boxed{\left\langle E_x\right\rangle = \frac{1}{8}E_{x1}\left(k_\perp\rho_e\right)^2 \sim T_e}$$

Finite Lamor radius effect

Physical Mechanism of O1-Mode Heating

Parallel electron velocity: $\mathbf{v}_{1z} = v_{1z} \cos \omega_e t \ \mathbf{z}$

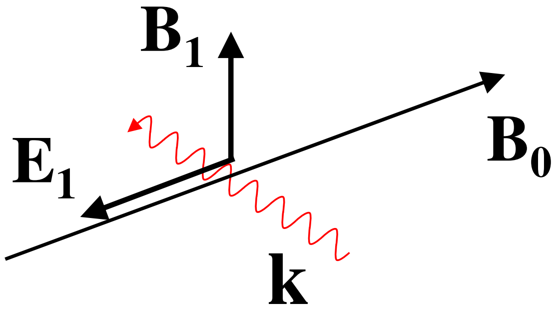

Lorentz force: $F_x = -e\mathbf{v}_1 \times \mathbf{B}_1 = -v_{z1} \dfrac{k_\perp}{\omega} E_{z1} e^{i2(\mathbf{k}\cdot\mathbf{r}-\omega t)}$

$$v_{z1} B_{y1} e^{i2(\mathbf{k}\cdot\mathbf{r}-\omega t)} = v_{z1} B_{y1} \left[\sum_{n=-\infty}^{\infty} i^n J_n\left(k_\perp \rho_e\right) e^{i(\omega_{ce}-\omega)t} \right]^2$$

If $\omega = \omega_{ce}$,

$$\langle F_x \rangle = F_{x1} J_1{}^2\left(k_\perp \rho_e\right)$$

Averaged Lorentz force is finite!

Since $k_\perp \rho_e << 1$,

$$\boxed{\langle F_x \rangle = \frac{1}{4} F_{x1} \left(k_\perp \rho_e\right)^2 \sim T_e}$$

Finite Lamor radius effect

How much is $k_\perp \rho_e$ in ITER?

- Wave frequency: $f = 170$ GHz
- Vacuum wavelength: $\lambda = c/f \approx 1.76$ mm
- Perpendicular wave number (assuming $k_\perp \approx k_0$): $k_\perp = 2\pi/\lambda \approx 3.56 \times 10^3$ m^{-1}
- Electron thermal speed at $T_e = 10$ keV:

$$v_{th} = \sqrt{2T_e/m_e} \approx 5.9 \times 10^7 \text{ m/s}$$

- Electron Larmor radius

$$\rho_e = v_\perp/\omega_{ce} \approx 5.5 \times 10^{-5} \text{ m} = 55\ \mu\text{m}.$$

Therefore,

$$\boldsymbol{k_\perp \rho_e} = (3.56 \times 10^3)(5.5 \times 10^{-5}) \approx \mathbf{0.20}.$$

The finite Larmor radius (FLR) effect is **small but not negligible**,

Absorption Coefficient

Fundamental O-mode (n=1)

It is absorbed efficiently via relativistic thermal effects and finite-Larmor-radius (FLR) corrections.

$$\alpha_\omega^{O(n=1)} \sim \frac{\omega_{pe}^2}{c\omega_{ce}}\left(\frac{v_{Te}}{c}\right)^2 \sim n_e T_e$$

n-th Harmonic modes (n ≥ 2)

At higher harmonics, collective plasma screening effects diminish, and the absorption is governed primarily by finite FLR effects.

$$\alpha_\omega^{X(n)} \sim \frac{\omega_{pe}^2}{c\omega_{ce}}\left(\frac{v_{Te}}{c}\right)^{2n-2} \sim n_e T_e^{\,n-1}$$

$$\alpha_\omega^{O(n)} \sim \frac{\omega_{pe}^2}{c\omega_{ce}}\left(\frac{v_{Te}}{c}\right)^{2n} \sim n_e T_e^{\,n}$$

For $v_{te}/c \ll 1$,
The X-mode α_ω is stronger than that of the O-mode absorption by a factor of $(v_{te}/c)^{-2}$.

Single Pass Absorption and Optical Depth

Absorbed power

$$P = P_0\left(1 - e^{-\tau}\right)$$

Optical thickness

$$\tau = \int \alpha_\omega \, ds$$

$\tau \gg 1$: Optically thick
$\tau \sim 1$: Optically grey
$\tau < 1$: Optically thin

- The single pass absorption increases with an increase in electron density
- It rapidly drops at cut-off density

2nd X-mode

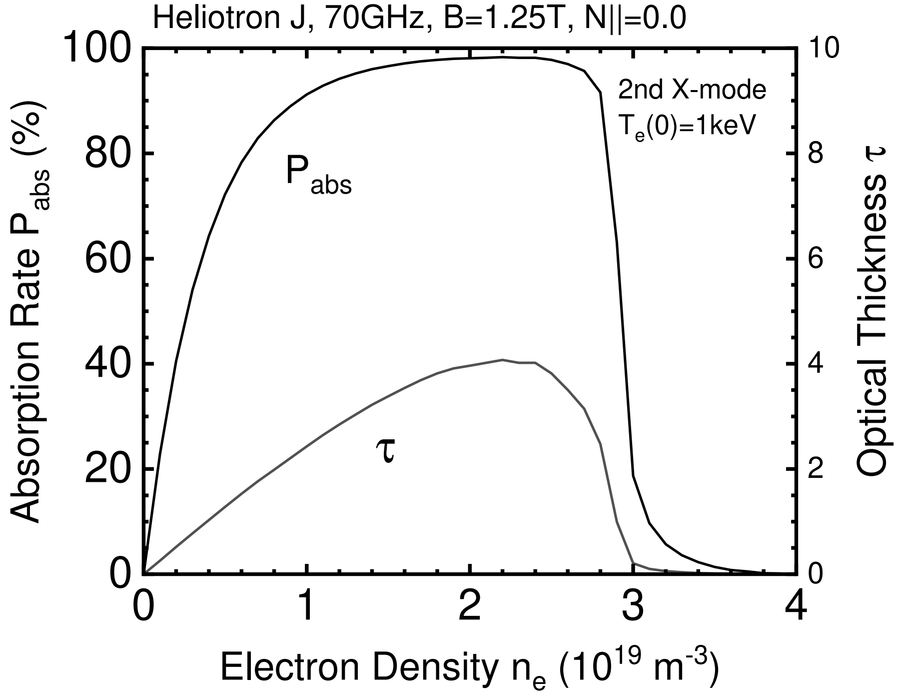

Comparison Table of Absorption Coefficient

Harmonic (n)	O-mode Absorption (α_ω^O)	X-mode Absorption (α_ω^X)	Application
$n = 1$ (Fundamental)	**Strong** (Effective at $\theta \sim \pi/2$)	Very Weak at $\theta = 90°$ (**Extremely strong at oblique θ**)	O1 is preferred for core heating at high densities.
$n = 2$ (2nd Harmonic)	Weak (Scales as $\sim T_e^2$)	**Strong** (Scales as $\sim T_e^1$)	X2 is widely used for ECRH/ECCD due to superb localized absorption.
$n = 3$ (3rd Harmonic)	Extremely Weak (Scales as $\sim T_e^3$)	Moderate/Weak (Scales as $\sim T_e^2$)	X3 is used in top-launch scenarios or very high-temperature regimes.

Ray Tracing Simulation

Ray Tracing Equation

Ray tracing (WKB/geometric optics) tracks EC beam trajectories using Hamiltonian ray equations:

$$\frac{d\mathbf{r}}{dt} = -\frac{c}{\omega}\frac{\partial D/\partial \mathbf{N}}{\partial D/\partial \omega}$$

$$\frac{d\mathbf{N}}{dt} = \frac{c}{\omega}\frac{\partial D/\partial \mathbf{r}}{\partial D/\partial \omega} \qquad D(\mathbf{r},\ \mathbf{N},\ \omega) = \det\left[N^2\mathbf{I} - \mathbf{NN} - \boldsymbol{\varepsilon}(\mathbf{r},\omega)\right]$$

- Use an array of non-interacting rays to simulate a Gaussian distribution in the far-field
  - Misses effects of diffraction and interference
- Gaussian beam codes keep effects of diffraction, astigmatism, and interference
  - When the beam focus lies inside the plasma, this model is needed
- Both approaches calculate the absorption as the rays or beam propagate, using linear warm plasma absorption models
  - This provides radial profiles of the wave heating and current drive

Ray Tracing Calculation

TRAVIS Code

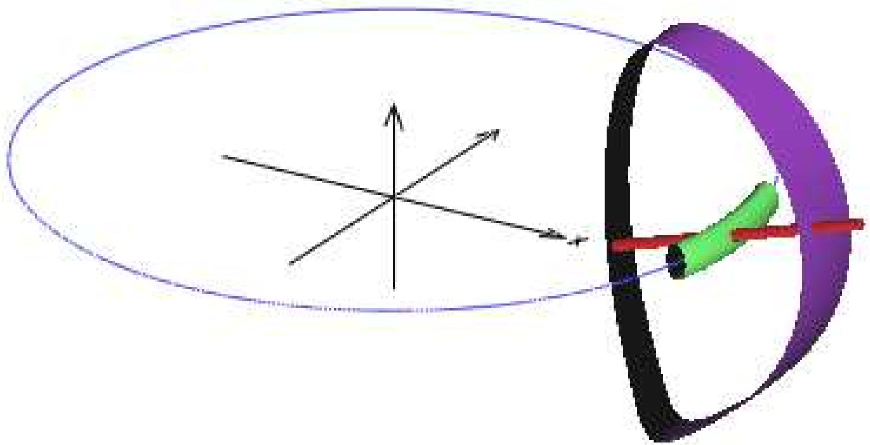

Outside O-mode launch
170GHz
B=5.3T

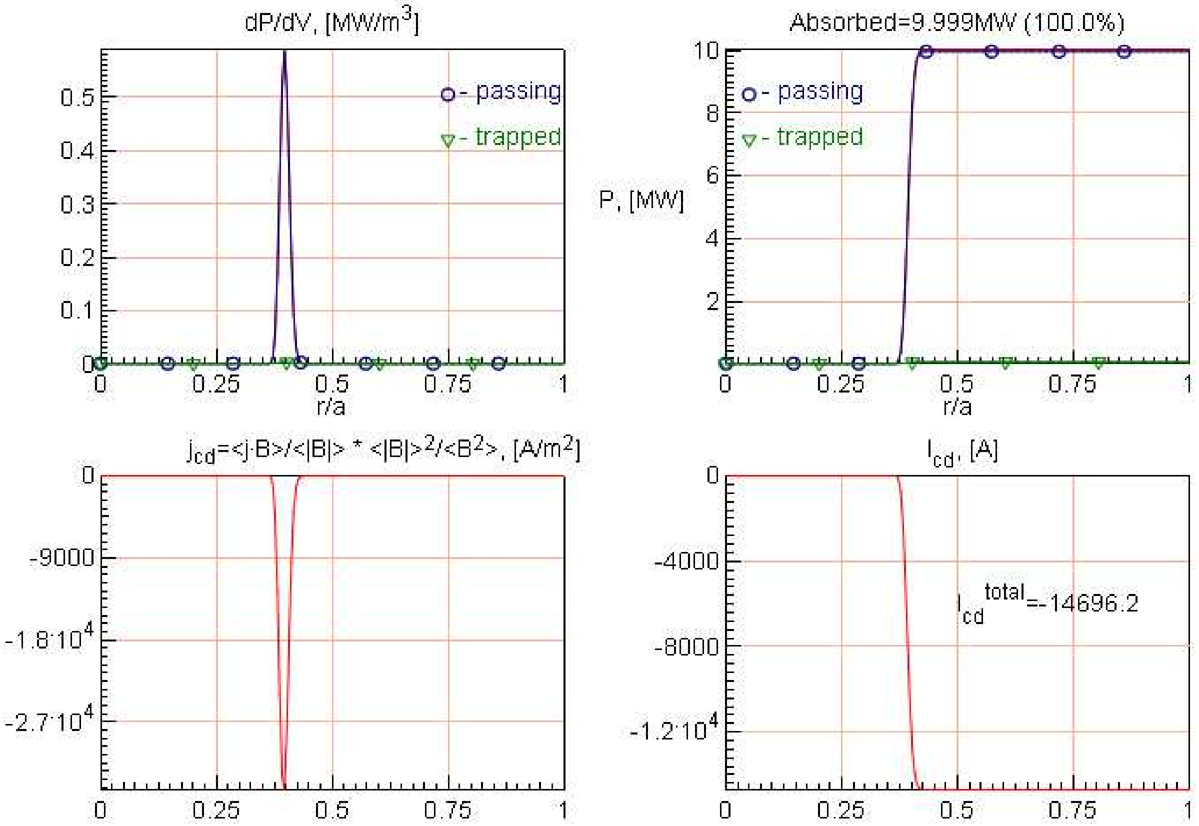

Ray Tracing Calculation

Fundamental O-mode

n_e=1.0x10^{20} m^{-3}

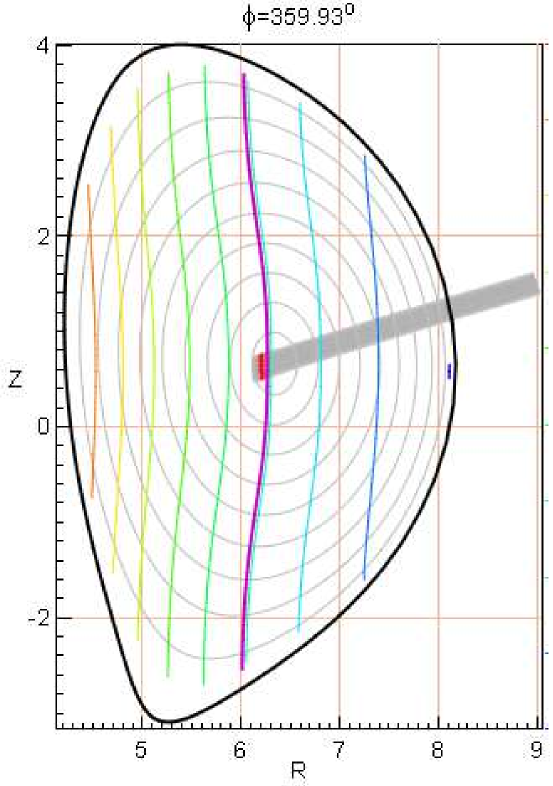

n_e=3.0x10^{20} m^{-3}

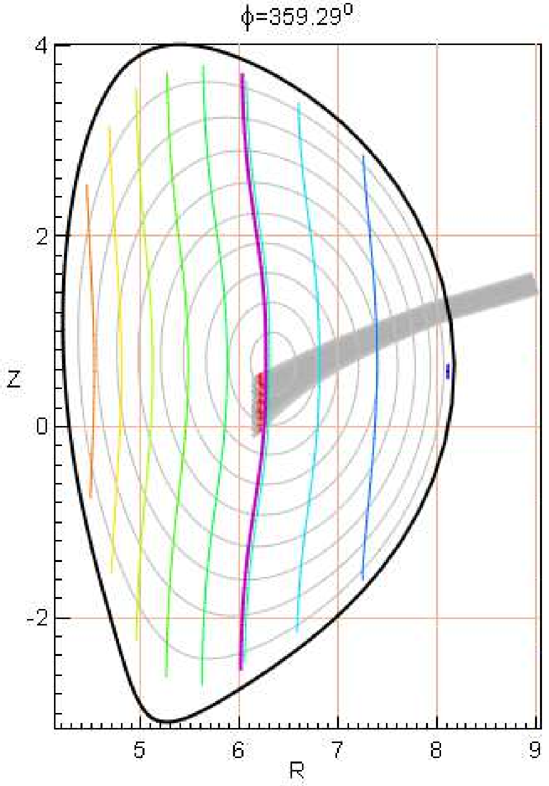

n_e=3.6x10^{20} m^{-3}

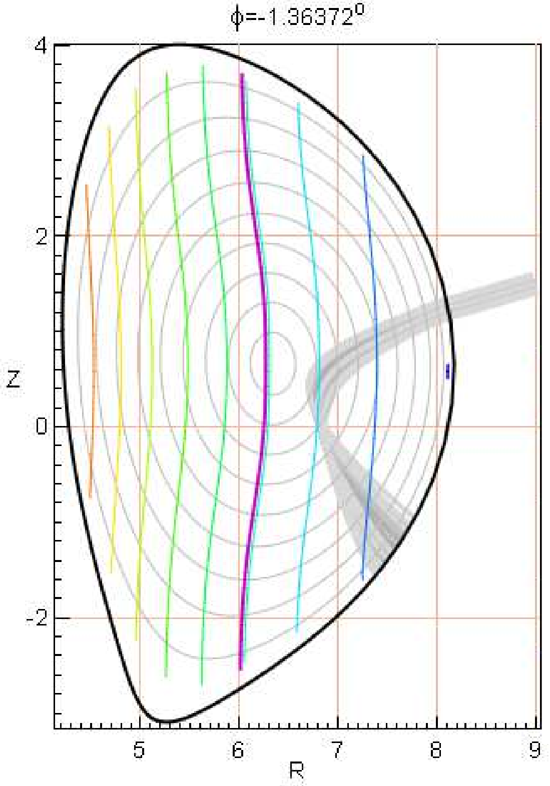

Deteriorating Effect of Plasma Density Fluctuations on EC Wave Quality

Refraction & Scattering:

- Density fluctuations cause local variations in dielectric permittivity and refractive index, which may lead to random scattering and refraction of the EC wave.

Beam Broadening:

- A focused Gaussian beam is subject to scattering and spreading out.
- Core and edge turbulence can broaden the beam width by 50% or more.

Beam Deflection and De-focusing:

- Fluctuations instantaneously deflect the beam path or misalign it from its intended trajectory.

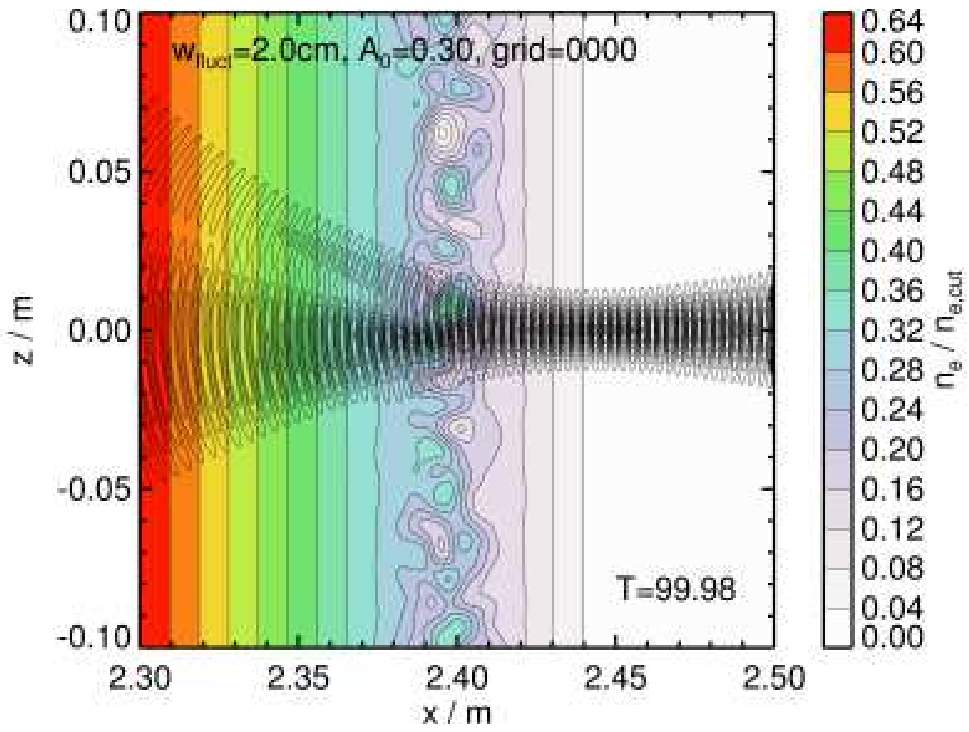

Alf Köhn, EPJ Web of Conferences 203, 01005 (2019)

Electron Cyclotron Current Drive (ECCD)

Why ECH/ECCD in Tokamaks?

- Localized and controllable current drive has important applications
  - Current profile control for optimization of tokamak performance
  - Stabilization of MHD modes
  - Tuning the shear profile in stellarators
- Electron cyclotron current drive has unique features which address these applications due to strong control over where the power is deposited
- In future DEMO tokamak reactors, non-inductive current is required to sustain plasma discharge for steady state

Physical Mechanism of ECCD – Fisch-Boozer Effect –

- Simply considering, electron cyclotron waves accelerate electrons perpendicularly, resulting in them not giving toroidal momentum
- However, the anisotropy in velocity space due to the EC waves with finite $N_{||}$ produces electron parallel momentum

Fisch-Boozer effect

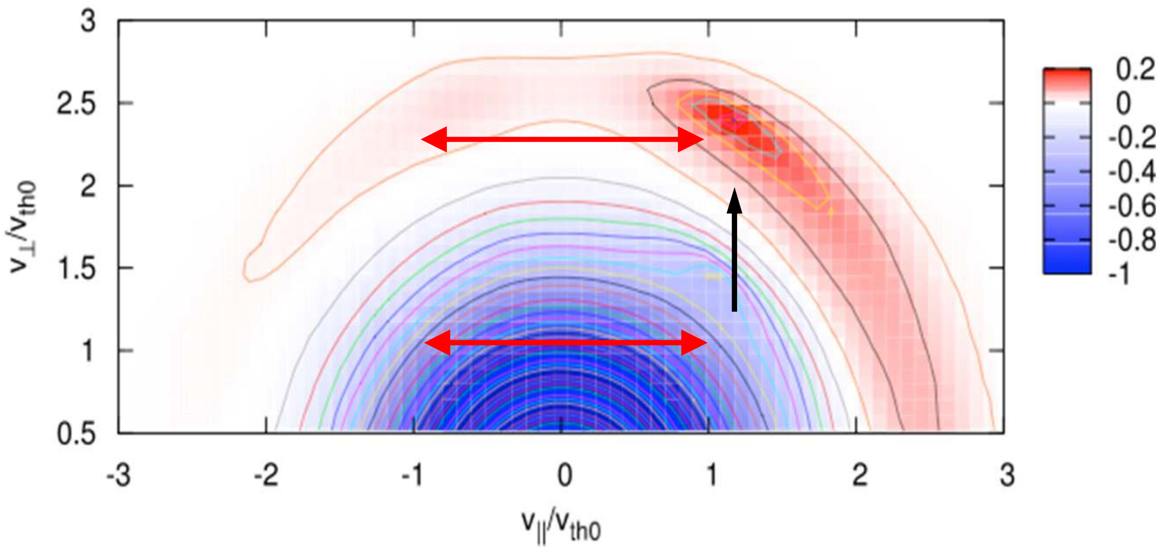

Linear Theory Predicts High ECCD Efficiency

- ECCD efficiency in linear theory

$$\eta_{EC} = \frac{j_{EC}}{P_{EC}} = \frac{4}{5+Z_{eff}} \frac{\mathbf{s}\cdot\nabla\left(v_{\parallel}/v_{th}\left(v/v_{th}\right)^3\right)}{\mathbf{s}\cdot\nabla\left(v/v_{th}\right)^2}$$

$$= \frac{3em\mathrm{v}_1^{\ 2}}{4\pi e^4 n_e \Lambda(5+Z_{eff})}$$

$$\boxed{\gamma_{EC} = \frac{I_{ECCD} n_e R}{P_{EC}} \sim \frac{T_e}{5+Z_{eff}}}$$

Fisch, Phys. Rev. Lett. 1980

- ECCD is **only a factor of 3/4 as efficient as LHCD**
- However, the efficiency is lower in experiments

Factors to Reduce ECCD Efficiency – Ohkawa Effect –

- There are some factors that reduce ECCD efficiency
  - Trapped particle effect (Ohkawa effect)
  - Incomplete single-pass absorption
  - Impurity contamination

Ohkawa effect Trapping

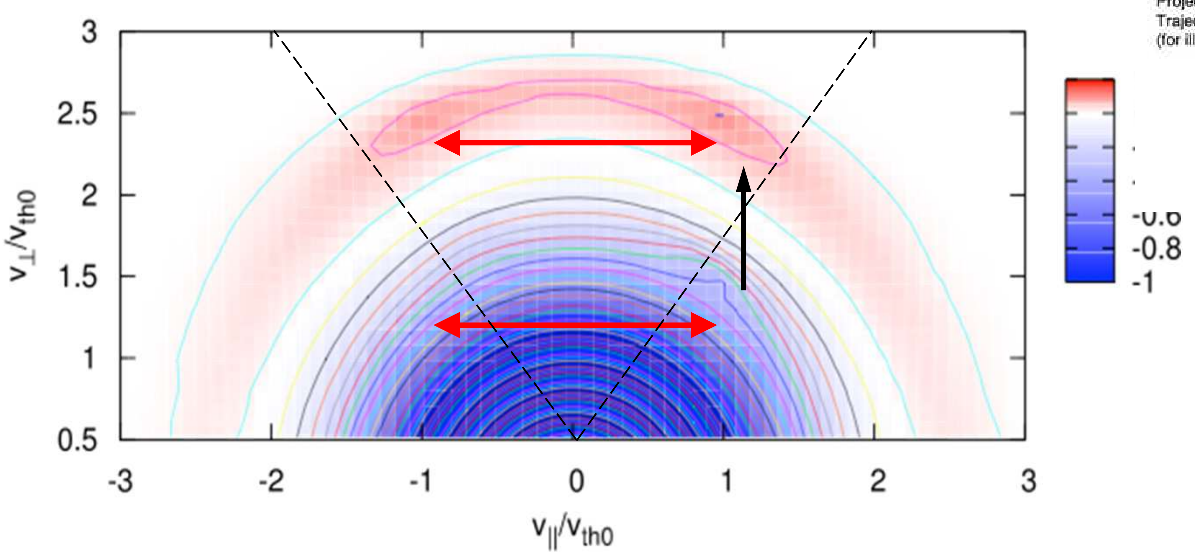

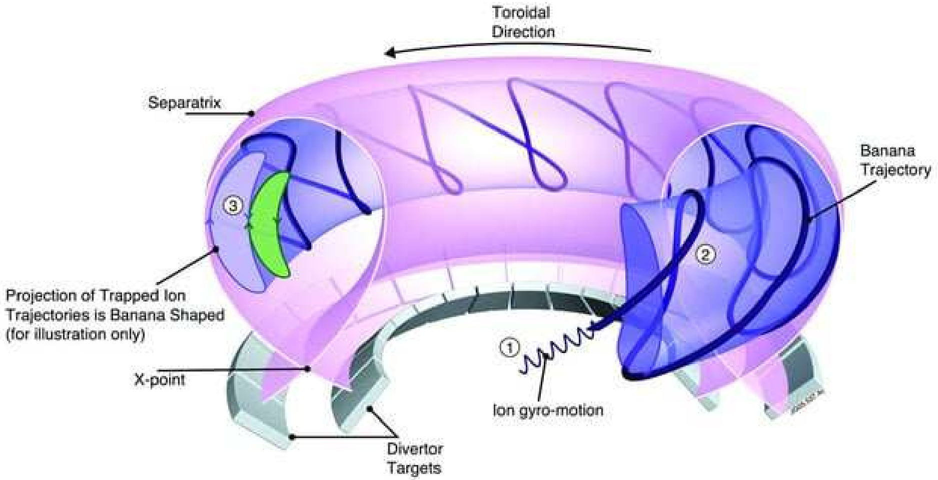

Brochard, Dynamics of ion-driven fishbones in tokamaks : theory and nonlinear full scale simulations, 2019

Top Launch ECCD in DEMO Reactor

- If the EC frequency ω is adjusted to be higher than the local cyclotron frequency, the waves are absorbed in high-energy electrons with high Doppler shift
- Modeling shows that using the top-launch approach can increase the ECCD efficiency by 50% or more

$$\gamma_{CD} = \frac{n_{20} R_m I_a}{P_W}$$

Low field side launch

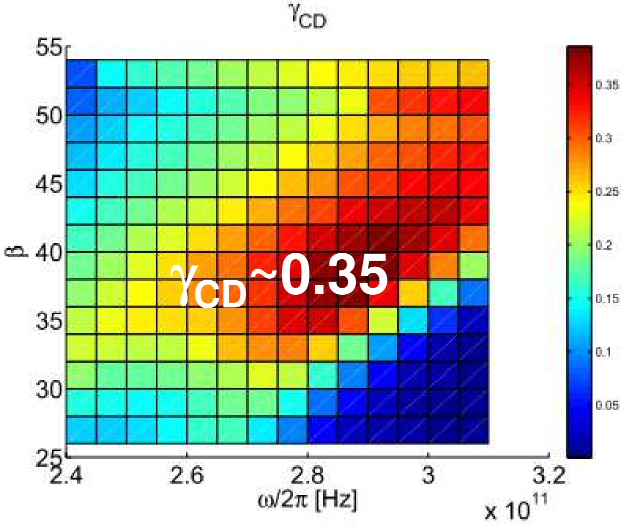

Top launch

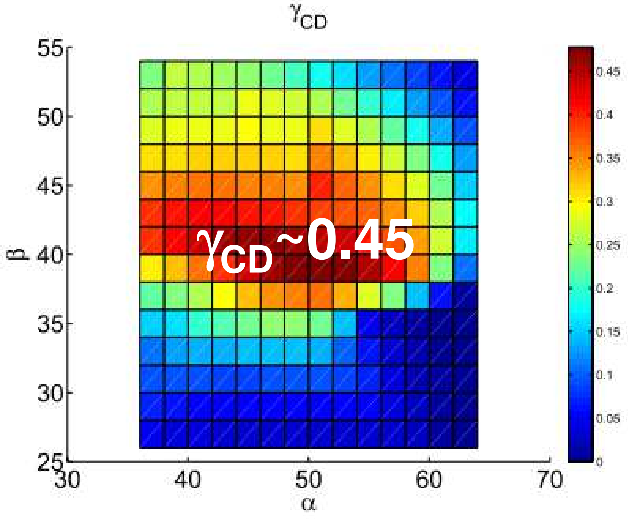

DEMO plasma, B=6.8T, f=290GHz

Poli, Nucl. Fusion (2013)

Improvement of ECCD Efficiency by Top Launch

- Top launch ECCD makes the efficiency more than doubled the conventional efficiency by tailoring the wave–particle interactions in velocity space
- Steering the EC waves to propagate nearly parallel to the resonance drives current more efficiently by (1) higher parallel velocity $v_{||}$ and (2) absorption at higher $v_{||}$.

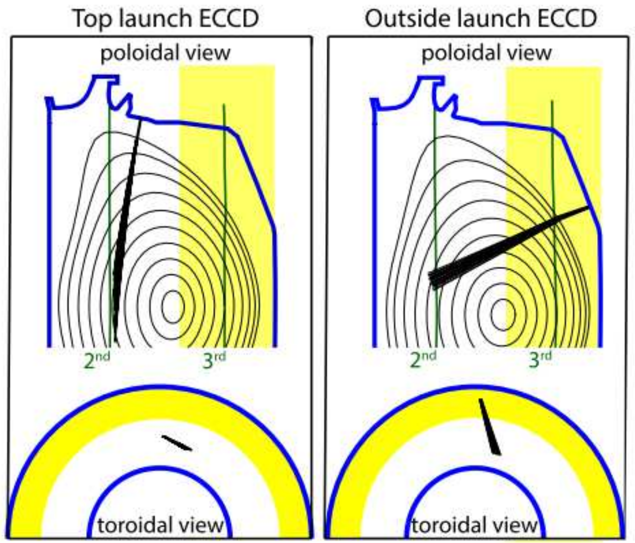

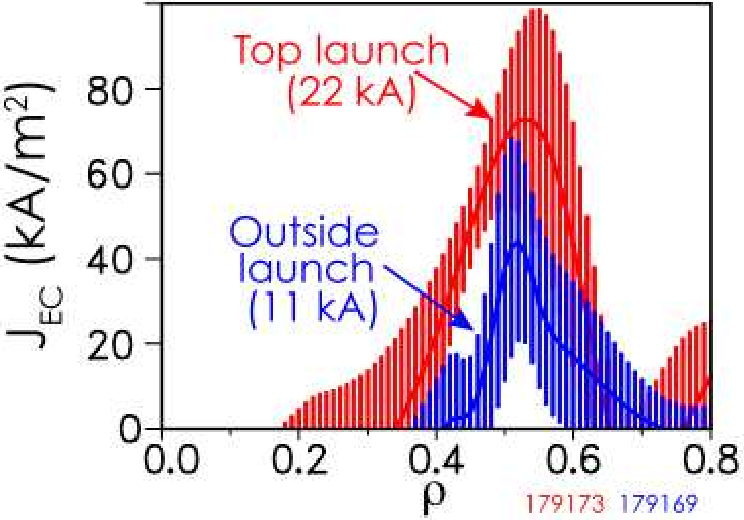

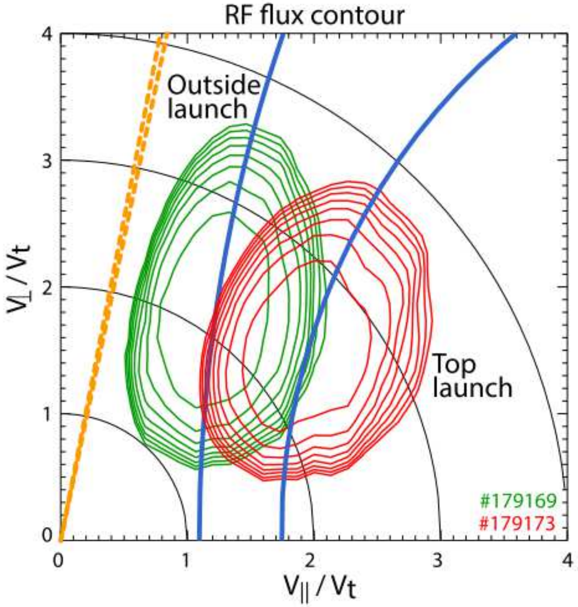

X. Chen, Nucl. Fusion 62 (2022) 054001

Applications

Stabilization of Neoclassical Tearing Modes by ECCD

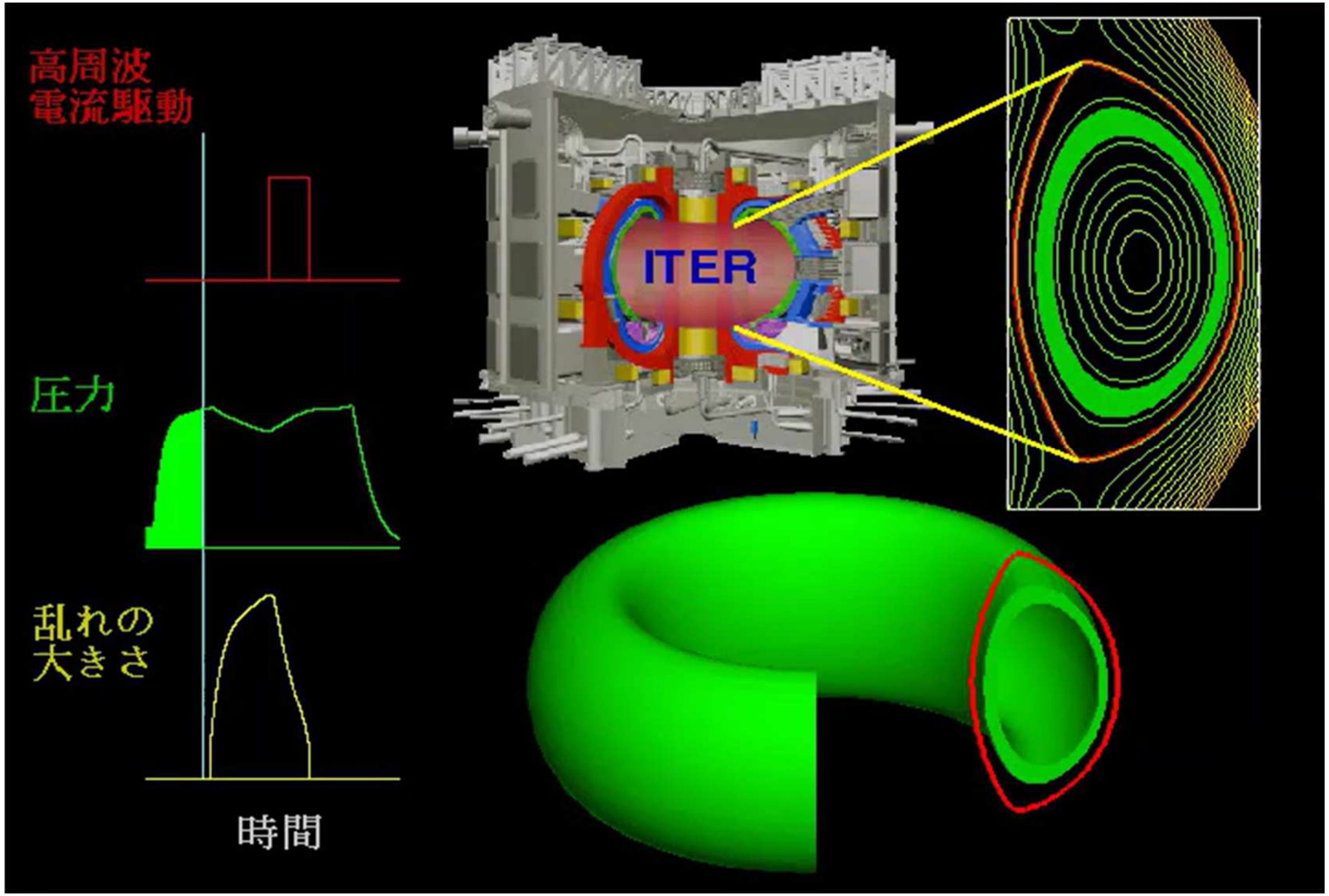

HL-2A: Real-time feedback control of TM

中核集团 CNNC 核工业西南物理研究院 Southwestern Institute of Physics

Courtesy of Mei Huang (SWIP)

- **In 2018, TM was suppressed in real time less than 50ms**
  - Resolution of magnet island position ±1cm
  - Response time of full scan range in poloidal direction of EC launcher: 50ms
  - Time of RT EFIT calculation: 600μs

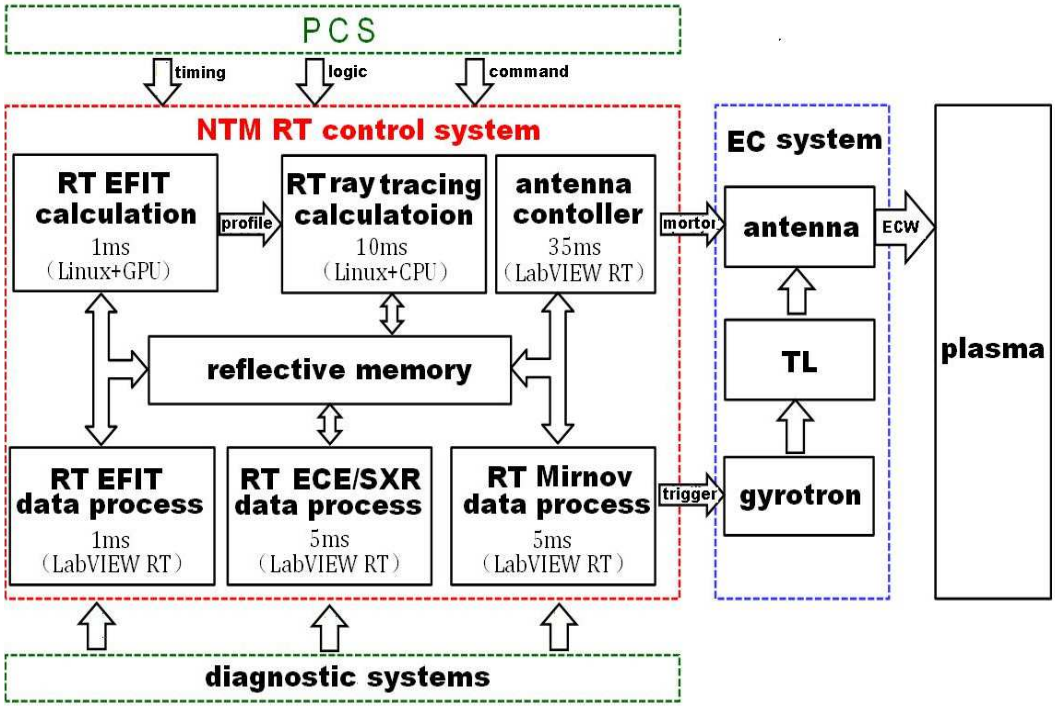

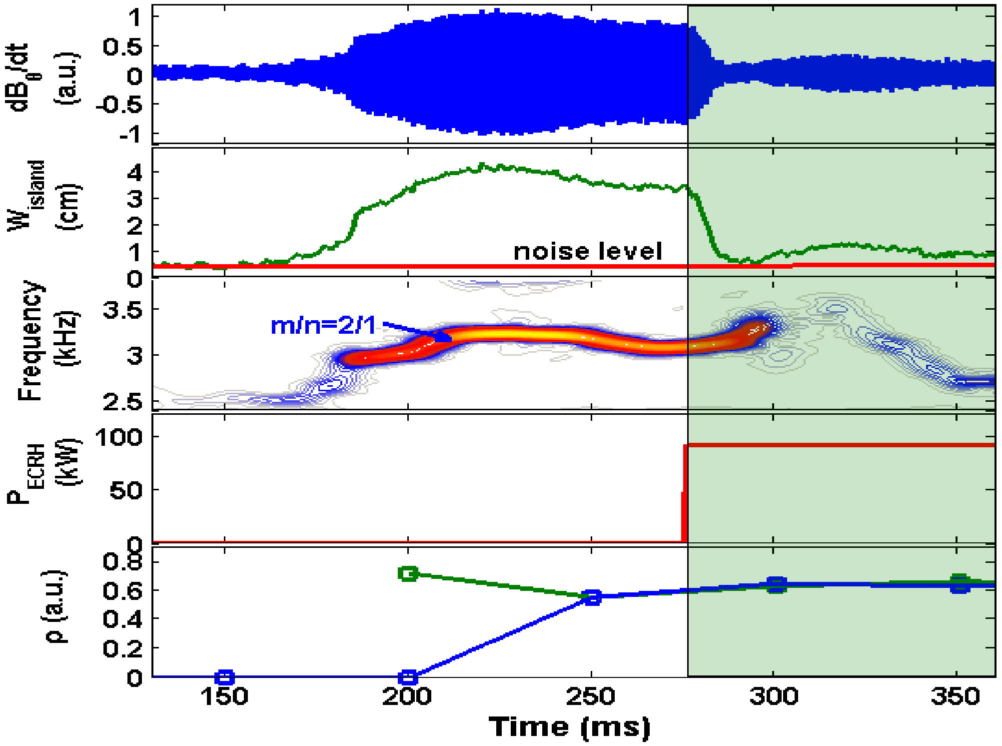

L.W.Yan, RSI 88 113504 (2017)

Modified Rutherford Equation

$$\frac{\mu_0}{\eta}\frac{dW}{dt} = \underbrace{k_c \Delta'(W)\left\langle|\nabla\rho|^2\right\rangle}_{\text{Classical}} + \underbrace{k_{BS}\mu_0 L_q j_{BS}\left\langle\frac{|\nabla\rho|}{B_p}\right\rangle\frac{W}{W^2+W_d^2}}_{\text{Bootstrap}} \underbrace{- k_{GGJ}\varepsilon_s^2\beta_p\frac{L_q^2}{\rho_s L_p}\left(1-\frac{1}{q^2}\right)\left\langle|\nabla\rho|^2\right\rangle\frac{1}{W}}_{\text{GGJ}}$$

$$\underbrace{-k_{pol}\varepsilon_s^{1.5}\beta_p\left(\frac{\rho_{pi}L_q}{L_p}\right)^2\left\langle|\nabla\rho|^2\right\rangle\frac{1}{W^3}}_{\text{Polarization}} \underbrace{- k_{EC}\mu_0\frac{L_q}{\rho_s}\left\langle\frac{|\nabla\rho|}{B_p}\right\rangle\eta_{EC}\frac{I_{EC}}{a^2}\frac{1}{W^2}}_{\text{ECCD}}$$

W : Magnetic island width in ρ coordinate

k_c=1.2, $\Delta'(W)$: Cylindrical model

$L_q = q / (dq/d\rho)$, ρ_s : Rational surface position

W_d : Finite $\chi_\perp / \chi_{//}$ effect (R.Fitzpatrick, 1995)

η_{EC} : Localized efficiency of EC current

I_{EC} : Total EC current

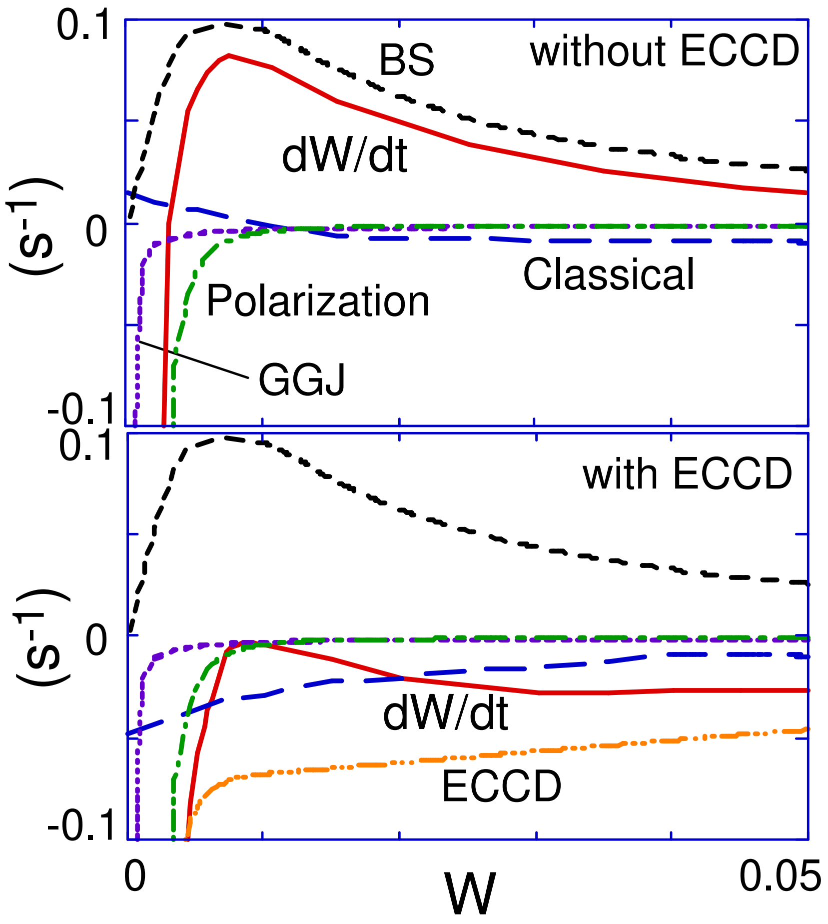

HL-3: Real-time control of 3/2 NTM

Courtesy of Mei Huang (SWIP)

■ Real-time neoclassical tearing mode (NTM) feedback control by ECH prelimilary realized

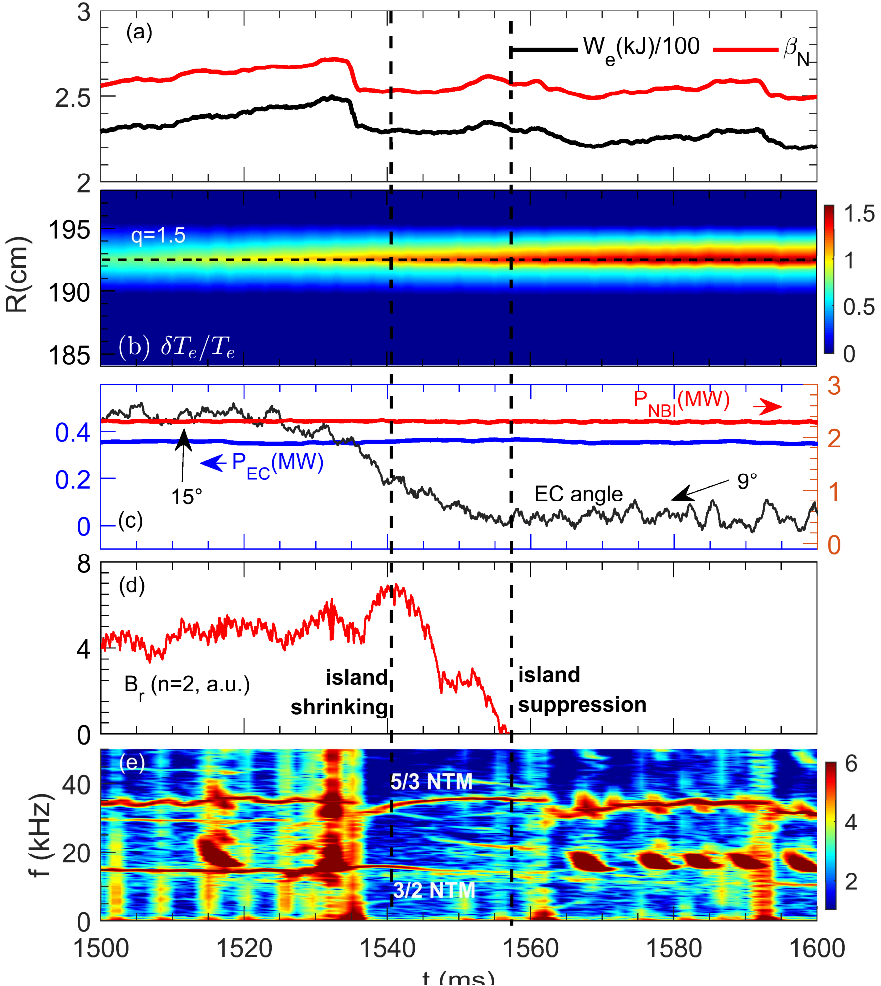

NTM identified by ECE → ECCD injected with particular angle → NTM suppressed

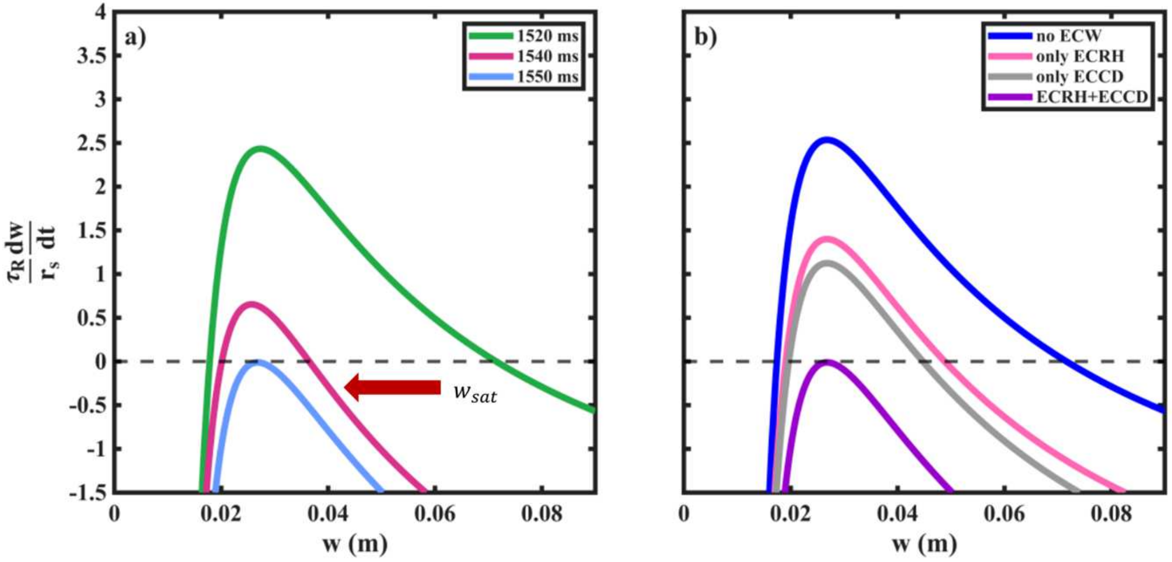

- Optimal EC antenna angle scanned;
- Real-time NTM identification and EC injection achieved, 3/2 NTM island shrank and finally suppressed when EC deposited near q=1.5 surface

Z. Y. Yin, NFPP accepted (2026)

Stabilization of Energetic Particle Driven MHD Instabilities by ECH/ECCD

- ECCD modifies the magnetic shear, stabilizing energetic particle modes and global Alfvén eigenmodes

Co-ECCD ($N_{||}$= +0.4)

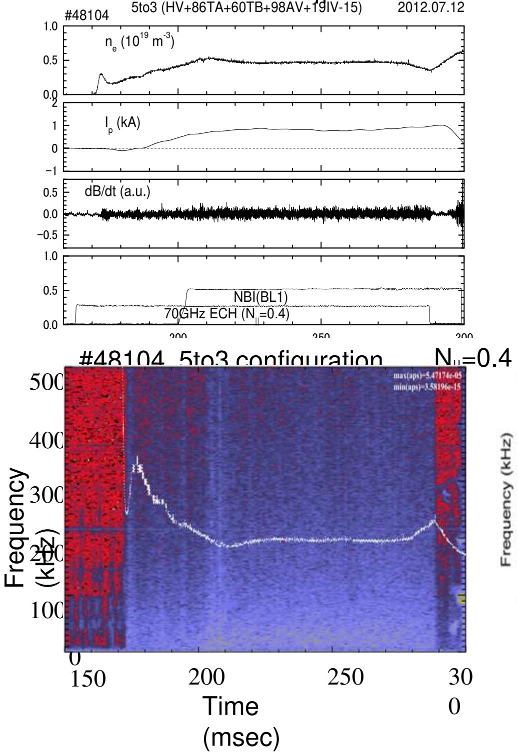

ECH ($N_{||}$=0.0)

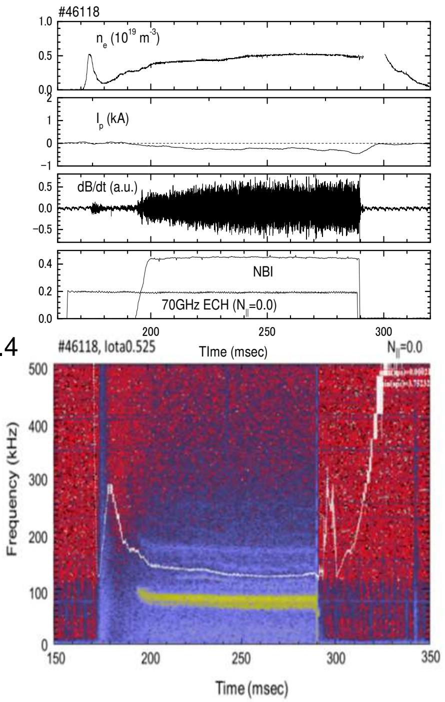

Ctr-ECCD ($N_{||}$= -0.3)

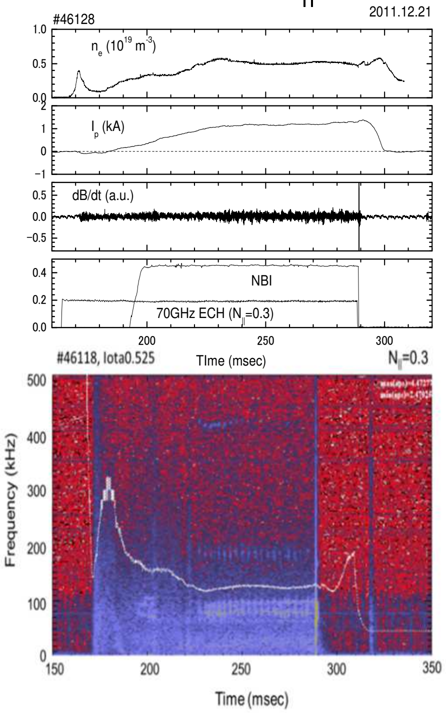

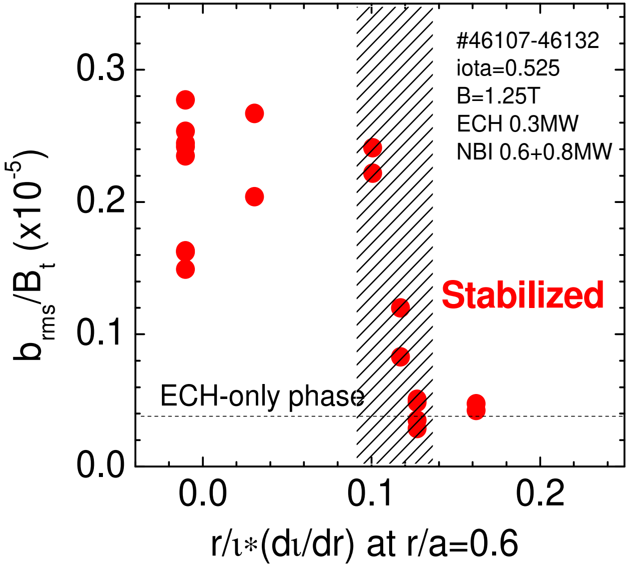

Nagasaki, Nucl. Fusion 2013
Yamamoto, Nucl. Fusion 2017, 2020
Zhong, Plasma Fus. Res 2024

HL-2A: Impurity transport enhanced by ECRH

核工业西南物理研究院
Southwestern Institute of Physics
中核集团 CNNC

Courtesy of Mei Huang (SWIP)

Z.Y. Cui, NF 58 056012 (2018)

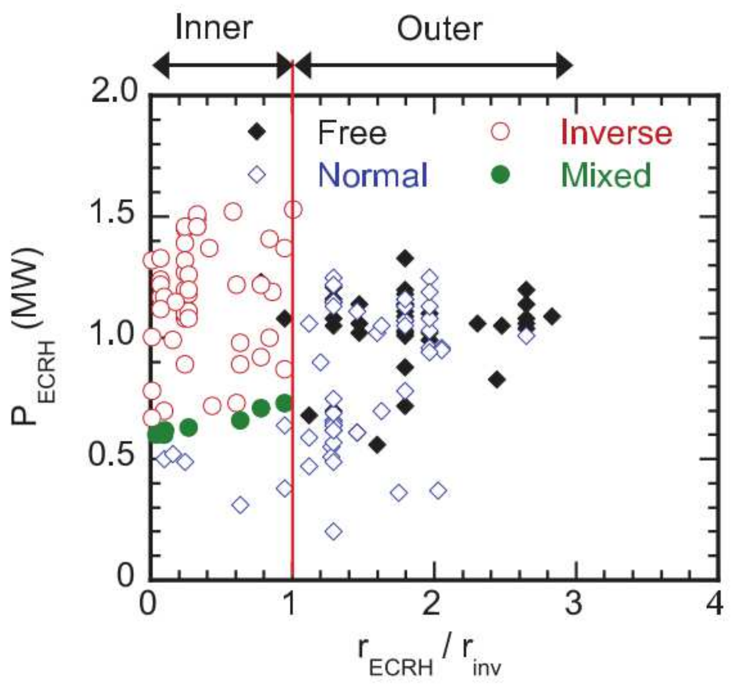

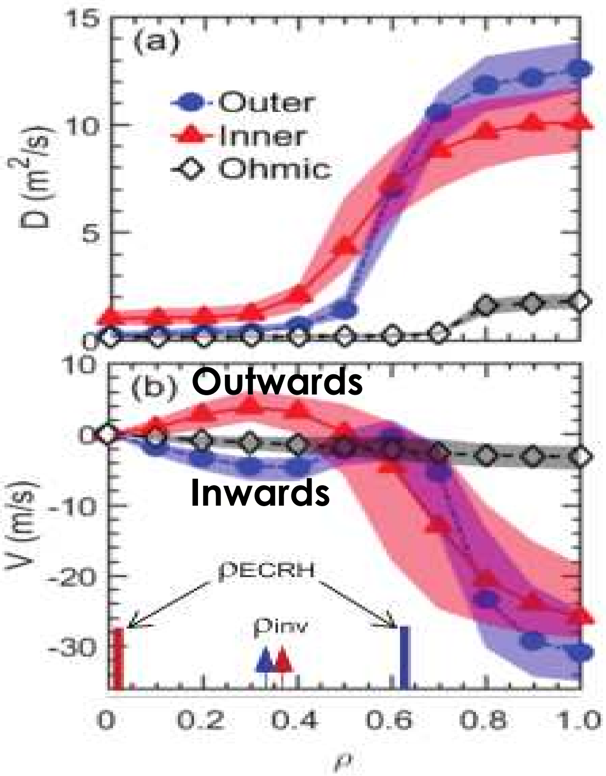

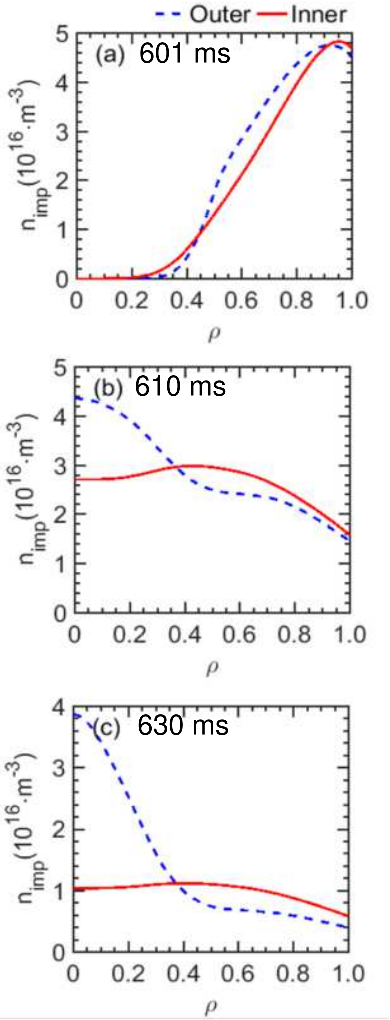

Inner-deposited (inside ST inversion radius) ERCH:

- Inverse sawtooth oscillation observed
- Outward convective velocity of Al impurity develops
- Al ion density profile flattened.

Plasma Start-up with Low Inductive Electric field in JT-60SA

- Plasma start-up experiments have been performed under low inductive electric field conditions.
- Trapped particle configuration enhanced EC-assisted breakdown, particularly for X2 heating, and enabled successful X2-only start-up.
- The lower power threshold for X2 start-up was found to be approximately 0.7 MW, set by the requirement for impurity burn-through rather than breakdown itself.

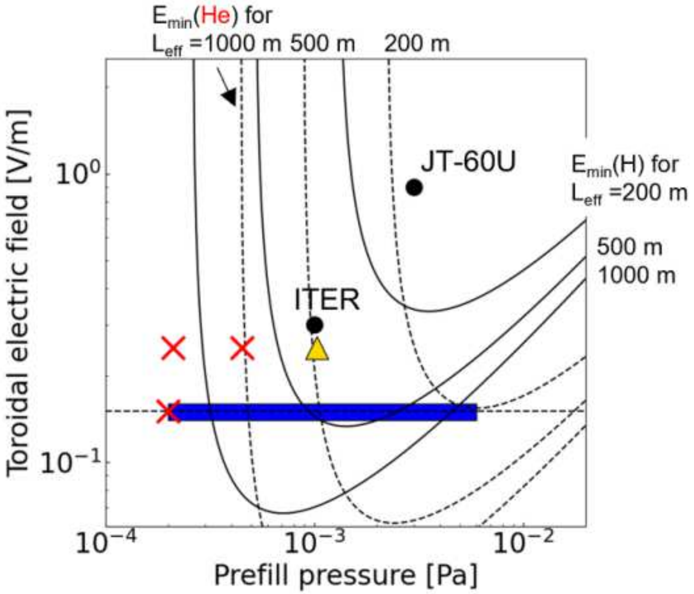

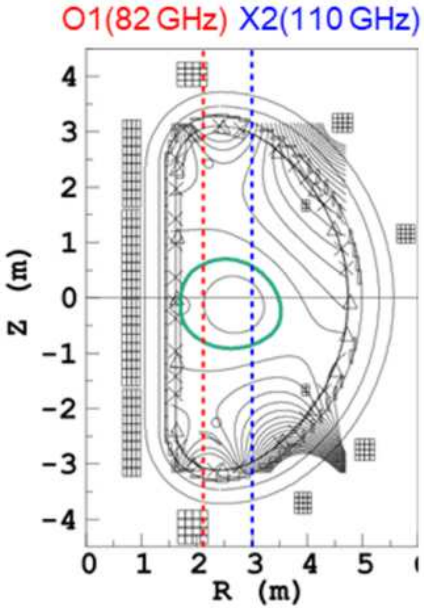

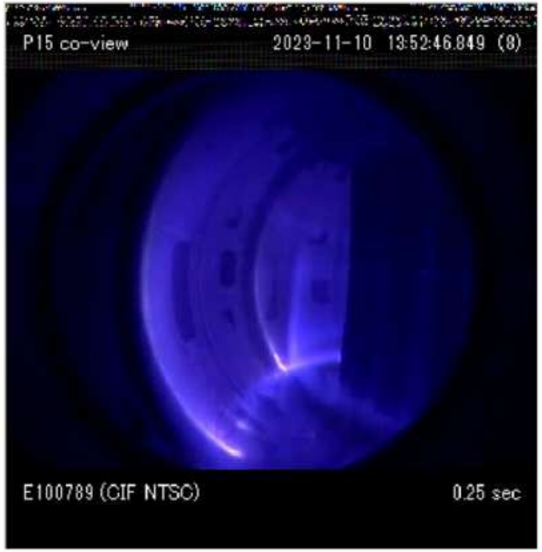

T. Wakatsuki , Nucl. Fusion 2026

Simulation of Plasma Start-Up in JT-60SA

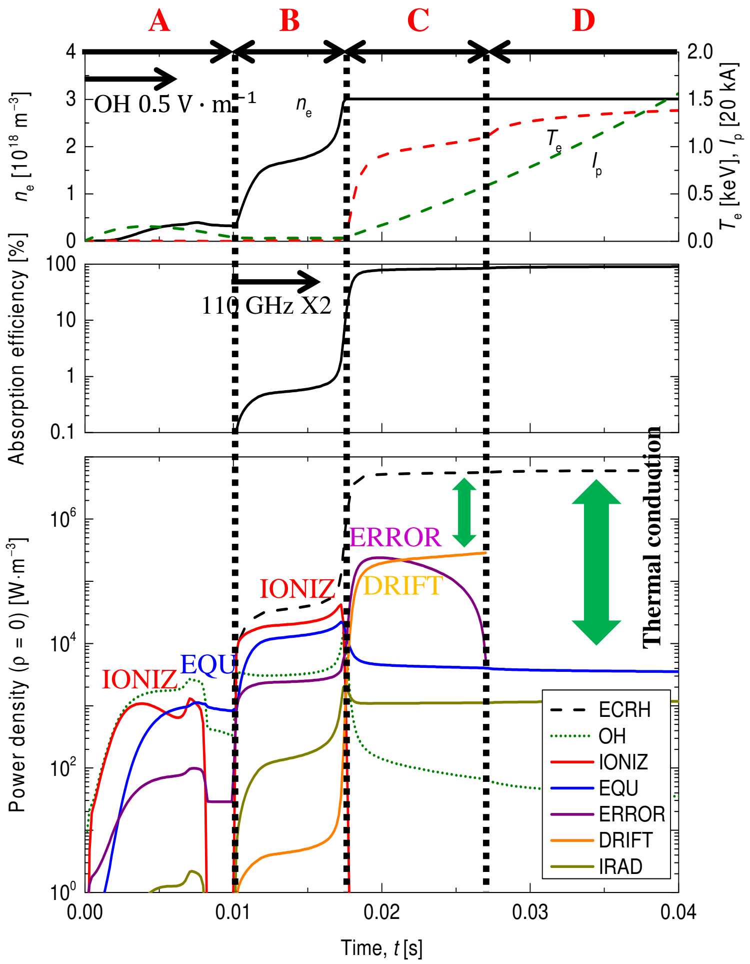

A) After onset of OH
- ✓ Gradual increase of n_e due to OH
- ✓ Ionization and equipartition loss are dominant

B) After ECRH injection
- ✓ Prompt increase of n_e due to ECRH
- ✓ ECRH power is consumed in the ionization
- ✓ T_e still remains around $5\ \mathrm{eV}$

C) $\boldsymbol{T_e}$ rise phase
- ✓ Positive feedback(ECRH absorption $\leftrightarrow$ T_e)
- ✓ ECRH absorption efficiency reaches nearly 100%
- ✓ Error field and drift losses are dominant
- ✓ Thermal conduction becomes dominant

D) Current ramp-up phase
- ✓ Thermal conduction is the dominant loss

Hada, Plasma Fus. Res. 2012
Hada, Fus. Sci. Technol. 2015

Wall conditioning by ECRH discharges

- Wall conditioning in the first operation campaign of W7 X consists of baking at 150 ° C, glow discharge conditioning (GDC) in helium (He) and ECH discharges.
- The recycling coefficient in H 2ECRH plasmas was reduced, and the pulse duration significantly was extended by He' recovery' ECRH plasmas.

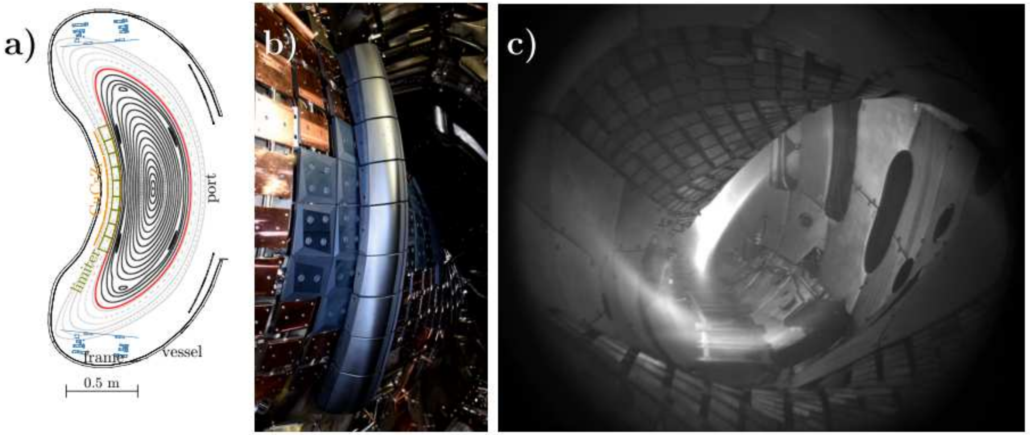

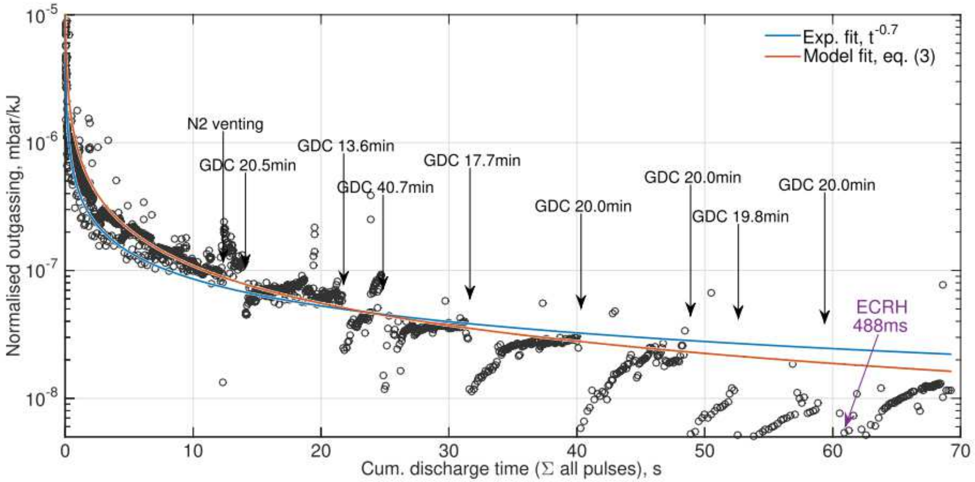

Wauters, Nucl. Fusion 2018

Recently Discussed Issues in EC Physics on ITER

1) **Non-perfect absorption in the early stages of plasma operation (during the ramp-up)**
   - The power density of the beam on the first wall from the upper launcher are high.

2) **Polarization control to ensure pure X-mode**
   - Not big for normal tokamaks, but could be an issue for ITER for long pulse operation.

3) **Location of additional resonances**
   - At the start of H-mode operation, the edge resonance cause X2
   - The edge resonance heating should be avoided

4) **Electron heated H-mode**

5) **Current drive and NTM stabilization control**

6) **EC wall conditioning**

Courtesy of P. deVries (ITER)

Conclusion

- ECH and ECCD are recognized as the main heating and current drive in magnetically confined fusion plasmas.
- The theory has been validated against experiment in considerable detail for parameters representative of today’s tokamaks and stellarators
- Much of the physics can be understood from the cold plasma dispersion relation for wave propagation and accessibility, and the kinetic theory for absorption and current drive
- Coupling to the plasma is not a technical issue
- Remaining physics issues
  - Effects of density fluctuations
  - Improvement of ECCD efficiency
  - Overcoming of cut-off density (heating by 3rd harmonic X-mode or 2nd harmonic O-mode, electron Bernstein wave heating)

Textbooks and Review Papers

Textbooks

- G. Bekefi, Radiation Processes in Plasmas, 1966, John Wiley & Sons, Inc.
- I. H. Hutchinson, Principles of Plasma Diagnostics, Cambridge
- J. Freidberg, Plasma Physics and Fusion Energy, Chapter 15
- Fusion Physics, IAEA Vienna, 2012, Chapter 6
- H-J Hartfuss, T. Geist, Fusion Plasma Diagnostics with mm-Waves, Wiley-VCH

Review papers

- M. Bornatici, et al., Nucl. Fusion 23 (1983) 1159 (EC absorption)
- N.J. Fisch, Rev. Mod. Physics 59, 175 (1987) (Current drive theory)
- V. Erckmann and U. Gasparino, Plasma Phys. Controlled Fusion 36 (1994) 1869 (EC physics and applications)
- T.C. Luce, IEEE Trans. Plasma Sci. 30, 734-754 (2002) (EC applications)
- R. Prater, Phys. Plasmas, 5, (2004) 2349 (EC physics)